Contract No:

This document was prepared in conjunction with work accomplished under Contract No. DE-AC09-08SR22470 with the U.S. Department of Energy.

Disclaimer:

Impact of Eliminating Mercury Removal Pretreatment on the Performance of a High Level Radioactive Waste Melter Offgas System

Paper #54

John R. Zamecnik and Alexander S. Choi
Savannah River National Laboratory, Aiken, SC 29808

ABSTRACT

The Defense Waste Processing Facility at the Savannah River Site processes high-level radioactive waste from the processing of nuclear materials that contains dissolved and precipitated metals and radionuclides. Vitrification of this waste into borosilicate glass for ultimate disposal at a geologic repository involves chemically modifying the waste to make it compatible with the glass melter system. Pretreatment steps include removal of excess aluminum by dissolution and washing, and processing with formic and nitric acids to: 1) adjust the reduction-oxidation (redox) potential in the glass melter to reduce radionuclide volatility and improve melt rate; 2) adjust feed rheology; and 3) reduce by steam stripping the amount of mercury that must be processed in the melter. Elimination of formic acid pretreatment has been proposed to eliminate the production of hydrogen in the pretreatment systems; alternative reductants would be used to control redox. However, elimination of formic acid would result in significantly more mercury in the melter feed; the current specification is no more than 0.45 wt%, while the maximum expected prior to pretreatment is about 2.5 wt%.

An engineering study has been undertaken to estimate the effects of eliminating mercury removal on the melter offgas system performance. A homogeneous gas-phase oxidation model and an aqueous phase model were developed to study the speciation of mercury in the DWPF melter offgas system. The model was calibrated against available experimental data and then applied to DWPF conditions. The gas-phase model predicted the Hg_2^{2+}/Hg^{2+} ratio accurately, but some un-oxidized Hg^0 remained. The aqueous model, with the addition of less than 1 mM Cl_2 showed that this remaining Hg^0 would be oxidized such that the final Hg_2^{2+}/Hg^{2+} ratios matched the experimental data. The results of applying the model to DWPF show that due to excessive shortage of chloride, only 6% of the mercury fed is expected to be chlorinated, mostly as Hg_2Cl_2, while the remaining mercury would exist either as elemental mercury (90%) or HgO (4%).

INTRODUCTION & BACKGROUND

The Department of Energy's Defense Waste Processing Facility (DWPF) at the Savannah River Site in South Carolina processes high-level radioactive waste (HLW) into glass for disposal in an off-site geologic repository. The DWPF began treating radioactive waste in 1996. Ultimately, the DWPF will immobilize the HLW portion of approximately 1.40×10^5 m^3 (37 million gallons,

Mgal) that is currently stored in underground tanks. As of January 2009, the DWPF has treated about $9.8x10^3$ m^3 (2.6 Mgal) of waste and produced 2680 canisters of HLW glass.

Most of the high level waste is a complex mixture of chemical and radionuclide wastes generated during the processing of reactor fuel and irradiated targets. Approximately $1.14x10^4$ m^3 (3 Mgal) of the $1.40x10^5$ m^3 (37 Mgal) of waste are sludge waste and $1.29x10^5$ (34 Mgal) are salt waste. The insoluble sludge, in the form of metal hydroxides, results from the neutralization of the acidic processing wastes. Neutralization to around pH 12 is required to prevent corrosion of the carbon-steel waste tanks. The sludge settles to the bottom of the waste tanks and contains insoluble radioactive elements including strontium, plutonium, americium, and curium. This sludge also contains the mercury used in the fuel and target processing in the form of HgO. The salt waste, which is soluble in the liquid, forms a supernate layer that contains most of the soluble radioactive element cesium.[1]

A simplified diagram of the DWPF treatment system is shown in Figure 1. The sludge waste is transferred into the Sludge Receipt Adjustment Tank (SRAT), where it is treated with formic acid, acidified with nitric acid, and concentrated. This treatment reduces the HgO to elemental Hg°, improves the rheology of the slurry, and adjusts the reduction-oxidation (redox) potential of the slurry. The redox adjustment is needed to optimize the melting of the sludge. The Hg° is stripped from the sludge by boiling and collected in a tank for further processing. Other byproducts are CO_2 from carbonate decomposition and NO_x from nitrate/nitrite reduction. The SRAT product is transferred to the Slurry Mix Evaporator (SME) where a borosilicate glass frit is added, followed by additional concentration. The SME product is verified to be acceptable before it is transferred into the Melter Feed Tank (MFT). The melter feed material in the MFT is then fed to the melter where the HLW glass product is made.

The glass melter is a joule-heated slurry fed melter which melts glass at 1100-1150 °C. A slurry of HLW and borosilicate glass frit is fed via a feed tube onto the top of the glass surface in the melter. The melter is equipped with Inconel™ resistance heaters in the vapor space to assist in vaporization of the water in the slurry feed and to combust offgases evolved from the slurry. The melter is purged with air and the offgas passes through a film cooler designed to minimize particulate build up in the offgas line and to cool the offgas from 450-725 °C to less than 350 °C.

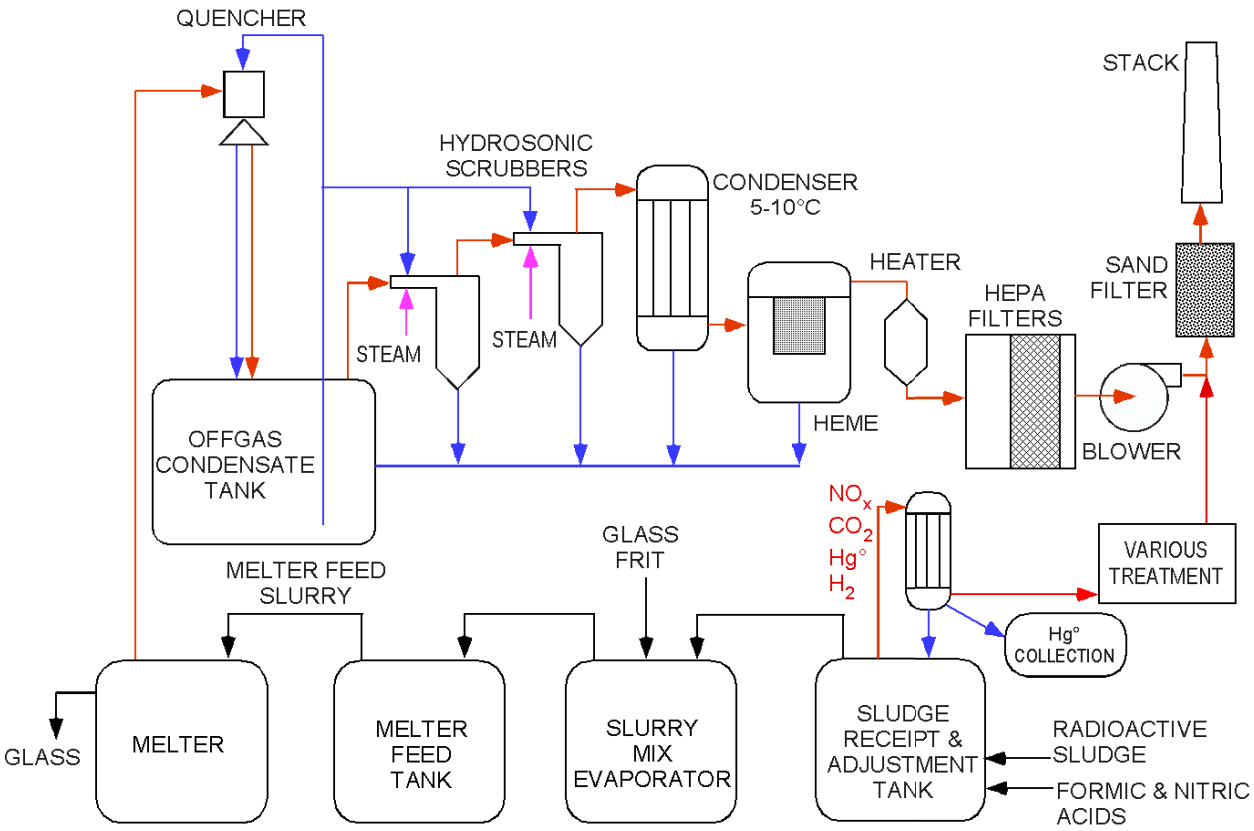

Figure 1 Flow Diagram of the DWPF Radioactive Waste Treatment System

After passing through the film cooler, the gas is then scrubbed in the quencher. The quencher is an ejector-venturi scrubber that reduces the gas temperature below the dew point, disengages most of the water vapor from the non-condensables, scrubs entrained solids, and allows semi-volatile salts (sulfates, nitrates, chlorides, borates) to coalesce. The quencher uses offgas condensate as the motive fluid. The offgas and condensate leaving the quencher enter the offgas condensate tank (OGCT) where the liquid and vapor disengage. The condensate is maintained at 40°C by a cooler.

The offgas from the OGCT is then passed through a series of two steam atomized scrubbers, or SAS (Hydro-Sonic Systems, Linden TX), which remove sub-micron and micron-sized particles. The SAS removes particulates by combining water and steam with the offgas in a region of turbulent mixing. The droplets of liquid formed are separated from the vapor in a cyclone separator. The condensate and condensed steam are returned to the OGCT.

The offgas leaving the SAS is passed through a 5-10 °C chilled water heat exchanger designed to separate the condensables from the offgas and reduce elemental mercury to its dew point. The DWPF operating permits allow elemental mercury to be emitted at this dew point; no further treatment is required. The separated condensables are returned to the OGCT. A demister and high efficiency mist eliminator (HEME) with atomized water sprays remove suspended liquid droplets from the non-condensable gases. The offgas is heated 10°C above its dew point to prevent condensation in the high efficiency particulate air (HEPA) filters. The final treatment is a

sand bed filter common to radioactive treatment plants. All condensates generated during this waste processing are recycled back to the waste tank farm.

In the feed pretreatment, the use of formic acid as a reductant results in the catalytic formation of hydrogen gas as a byproduct. Ruthenium, rhodium, and palladium present in the waste catalyze the formation of hydrogen from the formic acid. Because of its flammability, hydrogen measurement and control systems are required to guarantee safe operation. Because this is a nuclear facility, the reliability and redundancy of these systems is significantly greater than would be needed in non-radioactive operations. Remote maintenance is both difficult and expensive. Elimination of the formic acid treatment would greatly simplify the system and could result in significant increases in processing rate, which are both desirable. However, there are several issues to be resolved before this change can be made. Alternative methods to improve the slurry rheology and to adjust the redox will be required. Because the mercury will no longer be removed in the pretreatment, it will all be fed to the melter and ultimately need to be treated in the offgas system.

The Savannah River National Laboratory (SRNL) was asked to predict the impact of increased mercury concentration in the melter feed on the operation of the melter offgas system. The current specification for the product from the SRAT is that it contain no more than 0.45 wt% mercury. In typical operation from 1996 to 2008, this value averaged 0.1 wt%. The proposed operation without mercury removal could result in up to 2.5 wt% or more mercury. Without mercury removal in the pretreatment, removal in the melter offgas system is needed.

Mercury Measurement In Melter Offgas

Three very limited sources of melter offgas data are available on the behavior of mercury. These are the DWPF melter, an SRNL pilot-scale melter system,[2] and a small-scale system at the DOE Pacific Northwest Laboratory. The concentrations of chloride and mercury in these systems were significantly different, as shown in Figure 2. Past operation of DWPF has had Hg^0 in the pretreated sludge at less than 0.03 wt% up to 0.06 wt% while chloride has ranged from 0.007 to 0.018 wt%. Several data points are shown with Hg^0 as the target value of ≤0.1 wt% because the Hg concentrations were not measured. SRNL pilot-scale melter tests were conducted at about 0.09 wt% chloride and less than 0.01 wt% mercury. Tests in the ESCM melter at Pacific Northwest Laboratory had mercury levels similar to DWPF but the chloride values were much higher at 0.33 wt%. The proposed operation with no mercury removal for future batches is shown as a range from a measured Hg^0 concentration of 1.82 wt% to a possible high value of 2.5 wt%. Two different values are given for the chloride concentration – the actual chloride is about 0.01 wt% whereas the amount in a simulant is much higher at 0.11 wt% (due to having one simulant metal available only as a chloride). Figure 2 clearly shows that future operation will be in a region where no radioactive or simulant data is available.

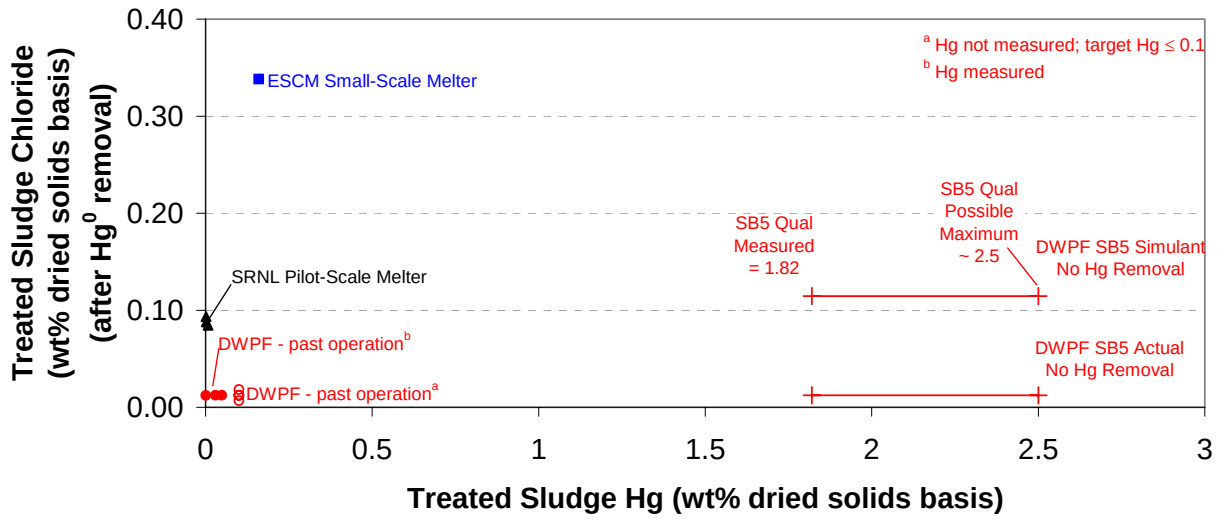

Figure 2 Chloride versus Hg in Various Sludges

DWPF Melter Offgas Deposits and OGCT Liquid

Deposits of solids on melter offgas system piping have occurred periodically throughout DWPF operation. Deposits have typically been found at the quencher inlet, the SAS inlet, in the vapor lines to the SAS, in the offgas condenser condensate line, and on the HEME filter. After about five years of radioactive operation, the steam to the SASes was stopped to reduce the amount of new water returned to the waste tank farm. Beginning at this time, plugging of the HEME filter increased significantly resulting in biannual replacement; previously the HEME filter had never been changed. Several years later, the steam to one SAS was restarted due to even worse plugging.

Melter offgas system solids deposit samples from the quencher inlet and SAS inlet were taken and analyzed.[3,4] The locations of these deposits are shown in Figure 3. An OGCT sample was also analyzed.[5] These deposits become significant enough to require periodic removal. The average concentration of mercury, chloride, and the most abundant elements in these samples are summarized in Table 1. Only soluble Cl was measured in the samples; the total was estimated from the measured soluble amount and the amount that would be present in Hg_2Cl_2 with the measured Hg values. The melter feed values are average measured values except 1) Cl was calculated from the sludge feed, and 2) Hg was calculated from the typical Hg removal of 0.1 wt% in the SRAT. The concentrations are also shown on a basis normalized against Fe which is the most abundant sludge species.

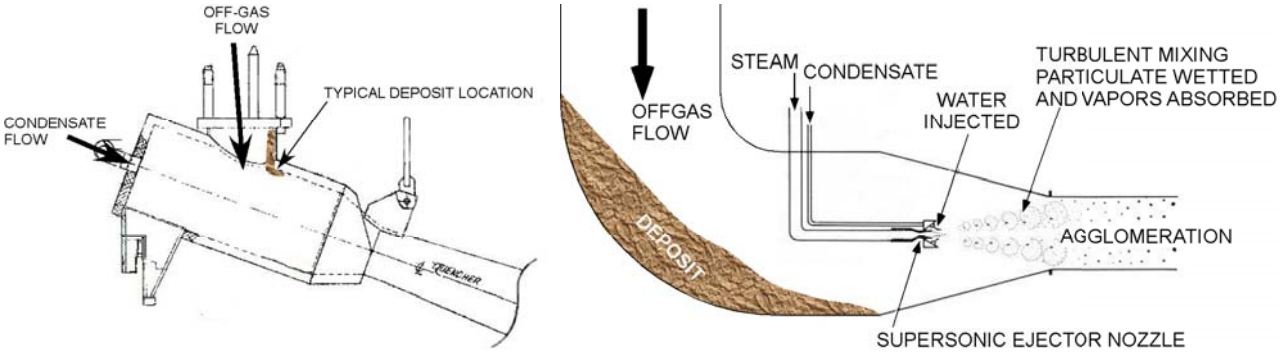

Quencher (not to scale) SAS

Figure 3 Locations of Quencher and SAS Deposits

Table 1 Typical Melter Feed and Offgas Deposit Species Concentrations

		Concentration (wt%)			Concentration (relative to Fe)		
Element	Primary Source	Melter Feed	Quencher Deposits	SAS Deposit	Melter Feed	Quencher Deposits	SAS Deposits
Total Hg	waste	0.04	0.14	4.8	0.5	1.4	80
Soluble Hg		-	-	0.4	-	-	6.5
Cl	waste	0.012	0.025	0.85	0.16	0.25	14
Soluble Cl		0.012	0.020	0.20	0.16	0.20	3.3
Si	frit	23	4.0	23	295	40	383
Na	waste, frit	8.8	4.7	3.0	113	47	50
Fe	waste	7.8	10.0	6.0	100	100	100
Al	waste	3.0	4.5	0.3	38	45	5.0
U	waste	2.8	5.4	0.2	36	54	3.3
Li	frit	2.3	0.2	0.1	29	2.0	1.7
Mn	waste	1.6	2.4	1.0	21	24	17
B	frit	1.5	0.3	0.3	19	3.0	5.0
Ca	waste	0.8	1.5	0.1	10	15	1.7
Mg	waste	0.7	1.1	0.3	9.0	11	5.0
Ni	waste	0.5	0.6	0.4	6.4	6.0	6.7
F	waste	0.13	0.15	0.5	1.6	1.5	8.3
S	waste	0.1	1.8	0.7	1.3	18	12

The Hg in the deposits was assumed to be mostly Hg_2Cl_2. Soluble mercury was measured only for the SAS deposits. X-ray diffraction (XRD) indicated that the SAS inlet samples contained significant amounts of crystalline Hg_2Cl_2. Qualitatively, the SAS deposits were grayer than the quencher deposits, consistent with the presence of calomel which disproportionates slightly to Hg° (grayish) and $HgCl_2$. The major chloride species in both deposit samples was Hg_2Cl_2. Fe, Si, and Na are expected to be the predominant species in the offgas due to particle entrainment. Species known to be most volatile are B, Cl, F, S, and Hg. The most volatile species either form vapors or what is called semi-volatile species. Semi-volatile species are usually chloride, sulfate, or borate salts that have relatively low melting points compared to glass. The data show that Hg, Cl, F, and S are relatively greater in the SAS deposits, which is consistent with their higher volatility.

The soluble Hg contents of the SAS deposits and OGCT liquid was about 6-10% and 5%, respectively, of the total mercury. This soluble Hg is expected to be $HgCl_2$, because $HgCl_2$ is the only likely mercury compound to have significant solubility in water (~0.26 mol/kg water @ 25°C).[6,7] Hg_2Cl_2 has an extremely low solubility (K_{sp} = 1.42 x 10^{-18} mol^3 kg^{-3} @ 25°C);[8] it is actually more likely to disproportionate into Hg° and $HgCl_2$:[9]

$$Hg_2Cl_2(s) = Hg°(\ell) + HgCl_2(aq) \qquad K = 2.35 \times 10^{-7} \text{ mol kg}^{-1}$$

The SAS deposits contained up to ten times the amount of mercury as found in the quencher deposits. The temperature at the quencher inlet is about 250-300 °C, whereas the SAS inlet temperature is about 45-60 °C. The quencher deposits contain relatively more entrained components than at the SAS because they are scrubbed out in the quencher. The pilot-scale work previously performed by SRNL had mercury feed concentrations too low to give any useful data on mercury speciation.

Engineering Scale Ceramic Melter (ESCM) at Pacific Northwest Laboratory

The ESCM melter at Pacific Northwest Laboratory was used to study mercury speciation in the offgas system.[10] The offgas mercury data collected during these tests are the most complete found for glass melter operation. The melter system was similar to DWPF and consisted of a slurry-fed joule-heated melter with a venturi scrubber (quencher), condensate or quench tank (OGCT), chilled-water condenser, and HEPA filter. The feed composition tested was similar to DWPF and the feed was treated with formic acid. Offgas system tests were conducted at several melter plenum temperatures and several air-inleakage rates.

Chloride was present in the ESCM feed at 12 times the mercury concentration. The Cl/Hg molar ratio in the SRNL pilot system was 67 to 436, whereas this ratio in DWPF has ranged from 0.55 to 2.2 in the past and is currently about 0.25. The proposed DWPF operation with higher mercury gives a ratio of 0.034. Therefore, the DWPF has operated with significantly less Cl than was tested in pilot-scale operations.

The ESCM melter offgas samples were filter, passed through a condenser, and then through three water-filled impingers. No mercury compounds were found on the filters, indicating that no solid Hg_2Cl_2 had been formed. The mercury in the impingers, and also in the condensate tank liquid, were speciated qualitatively by assuming mercury in the solids was Hg_2Cl_2, while soluble mercury was $HgCl_2$. The identity of the solid mercury species was verified by XRD. The splits of Hg species between Hg_2Cl_2 and $HgCl_2$ for five tests are shown in Table 2. The DWPF deposit sample ratios are also shown. No evidence of HgO was found in the offgas or condensate.

Table 2 ESCM Melter Offgas Samples

Test	Air Inleakage (kg/h)	Plenum Temp. (°C)	Impinger Samples (wt%)		OGCT Samples (wt%)	
			Hg_2Cl_2	$HgCl_2$	Hg_2Cl_2	$HgCl_2$
1	0.73	750	86	14	89	11
2	6.8	750	38	62	90	10
3	0.73	550	33	67	50	50
4	0.76	740	82	18	NA	NA
5	0.76	740	85	15	NA	NA
			SAS Deposit		**OGCT Sample**	
DWPF:	~750		90-94	6-10	95	5

For all the data at about 750 °C plenum temperature, Hg_2Cl_2 accounts for about 85-95% of the total mercury species found except for Test 2, which had anomalous results for the impinger samples that did not agree with the OGCT samples. In Test 3 at 550 °C plenum temperature, both the impinger and OGCT samples had significantly more of the more oxidized $HgCl_2$ present. Higher plenum temperature appears to favor formation of the less oxidized mercury compound Hg_2Cl_2.

The ESCM tests showed that the concentration of elemental mercury in the vapor phase was always approximately equal to the saturation vapor pressure at the prevailing temperature, even though no elemental Hg liquid was ever found in the offgas system. The gray color of the calomel and other solids samples was probably due to surface Hg^0 from disproportionation. This surface Hg^0 appears to exert the full Hg^0 vapor pressure. In fact, even when the melter was not being fed, the vapor above the condensate remained saturated with Hg^0.

Gas-Phase Oxidation Literature

Numerous papers have been written on the gas-phase oxidation of elemental mercury, primarily in coal-fired power plant emissions. In power plants, the mercury and chlorine concentrations in the flue gases are significantly lower than in the melter offgas systems of interest. Power plant mercury emission levels are typically in the range 0.1 to 4 ppbv (1-30 $\mu g/m^3$)[11] and waste incinerator levels may be up to about 400 ppbv.[12] Mendelsohn and Livengood[13] have reviewed a substantial portion of the literature on mercury chemistry in flue gas. Most papers divide the Hg emissions into insoluble (Hg^0) and soluble ($HgCl_2$), but generally ignore the insoluble Hg_2Cl_2. The goal for mercury oxidation in power plant flue gases has been oxidation to the soluble $HgCl_2$ that can be scrubbed from the gas. This goal is contrary to that for DWPF where collection of mercury as the insoluble Hg^0 metal might be preferred.

Homogeneous Oxidation

The homogeneous reaction schemes are all similar, but none have been found to be universally applicable to all combustors. For these mechanisms, chlorine atoms (Cl) are assumed to be in excess compared to mercury. The concentration of SO_2 present is usually higher than both Cl and Hg. The primary reaction step in the oxidation is the formation of HgCl from Hg atoms and Cl atoms in the presence of a stabilizing collision partner M in Reaction (1):[12,14-16]

$$Hg^0 + Cl + M \rightarrow HgCl + M \qquad k_1 = 6.0 \times 10^{-11}\ cm^3\ molecule^{-1}\ s^{-1} \qquad (1)$$

The following subsequent reactions are slower. Reactions (2)-(5) are independent of temperature. The rate constant for Reaction (6) is at 125 °C.

$$HgCl + Cl + M \rightarrow HgCl_2 + M \qquad k_2 = 4.0 \times 10^{-12}\ cm^3\ molecule^{-1}\ s^{-1} \qquad (2)$$

$$HgCl + Cl_2 \rightarrow HgCl_2 + Cl \qquad k_3 = 1.2 \times 10^{-11}\ cm^3\ molecule^{-1}\ s^{-1} \qquad (3)$$

$$Cl + Cl + M \rightarrow Cl_2 + M \qquad k_4 = 5.5 \times 10^{-33}\ cm^3\ molecule^{-1}\ s^{-1} \qquad (4)$$

$$HgCl + HgCl \rightarrow Hg_2Cl_2 \qquad k_6 = 4.2 \times 10^{-10}\ cm^3\ molecule^{-1}\ s^{-1} \qquad (5)$$

$$HgCl + HCl \rightarrow HgCl_2 + H \qquad k_5 = 6.3 \times 10^{-13}\ cm^3\ molecule^{-1}\ s^{-1} \qquad (6)$$

Reaction (3) is slow due to the low concentration of Cl_2 present under conditions where there is significant Cl present. The reactions of Hg^0 with Cl_2, HCl, O_2 and O are significantly slower.

Sliger[12] found that the homogeneous oxidation was primarily governed by the formation of Cl from HCl, the rate at which the hot offgas was quenched (cooled), and by the presence of background gases involved in competing reactions. These authors also mention the fly ash or carbon mediated reaction where HCl forms Cl_2 that can then react with Hg at temperatures lower than 300 °C. The importance of Cl formation from Cl_2 has been debated.

Senior[17] suggests that a pathway through HgO may be important in systems with low chlorine concentrations, but Sliger[12] found that no HgO was formed in the absence of HCl in their test gas. Hall[18] has suggested a mechanism with HCl and O_2 as important reactants. Edwards[19] has included oxidation by O_2 in modeling although it apparently has little effect on the overall oxidation. Models by Niksa[20] and Edwards[19] did not predict well the oxidation at less than ~700 °C. Sliger[12] predicted the oxidation was limited to the range 400-700 °C because there were too few Cl radicals at low temperature, while Hg^0 was favored at high temperature. They also noted that virtually all of the oxidation reaction occurred inside their sample probe where cooling at 5400 K/s from about 900 °C occurred. They developed models that showed the extent of Hg oxidation and the equilibrium amount of oxidation during the quench. Complete oxidation was predicted in 60 ms. The kinetically-controlled oxidation extent was only around 40% and was limited by the availability of Cl radicals. Fry[21] has reported that oxidation increased at higher quench rates. The species NO, NO_2, and SO_2 have been shown to have varying effects on the mercury oxidation rate.[18,20,22-25] NO and SO_2 have generally been found to inhibit oxidation of Hg^0, but not in all cases.

Heterogeneous Oxidation

Schofield[26-28] has hypothesized that the main mechanism of mercury oxidation in power plant emissions occurs heterogeneously on the fly ash present and on equipment surfaces. Numerous researchers have reported the difficulty in measuring the rate of homogeneous oxidation due reactions on the surfaces of their test equipment.[12,29-31] Laudal[32] has reported that fly ash can have a large effect on speciation. Senior[33] suggests that Cl_2 formed from HCl on the fly ash surface can oxidize Hg. Edwards[19] states that heterogeneous reactions are probably dominant at lower temperature – their model drastically under-predicted mercury oxidation below 630 °C.

Schofield proposed a mechanism that involves the interaction of mercury with surfaces. The surface intermediates HgO, $HgSO_4$, and $HgSO_4$•HgO are formed that then react with HCl to form $HgCl_2$. This mechanism does not require Cl_2. The presence of surface reactions in the DWPF melter system is not known. The residence time before the quench is about 0.5 s, and the amount of particulate is significantly less than the amount of fly ash in a power plant.

Oxidation in Aqueous Solutions

Most of the literature on aqueous oxidation concerns environmental systems such as lakes and rivers. The oxidation of elemental mercury by dissolved oxygen in the presence of chloride anions has been examined by several researchers. Other literature has addressed the unexpected oxidation of Hg^0 in the Ontario Hydro sampling train, which uses a chloride solution to scrub oxidized mercury (Hg^{2+}).[34] The oxidation in this sample train will be briefly discussed as it pertains to the oxidation of mercury in a melter offgas system. Elemental mercury in oxidizing

acids such as HNO_3 will be oxidized and dissolve to some extent to form Hg^{2+}. Oxidation by hypochlorite and chlorite have also been reported.[35,36]

Oxidation in Dilute Aqueous Solutions

Magalhães[37] studied oxidation of metallic Hg^0 in aqueous solutions containing NaCl. These tests were performed in agitated vessels open to the atmosphere. The reaction was monitored by following the concentration of the product $HgCl_4^{2-}$ (Hg^{2+}). $HgCl_4^{2-}$, the dichloride complex of $HgCl_2$, is the expected product with a large excess of Cl^-. Eventually the concentration of $HgCl_4^{2-}$ was found to decrease. At this time, the metallic Hg droplets lost their characteristic brightness and started to become white on the surface. Both the drop in $HgCl_4^{2-}$ and the white color were attributed to the formation of calomel on the surface of the Hg^0 droplets:

$$HgCl_4^{2-}(aq) + Hg^0(\ell) = Hg_2Cl_2(s) + 2\ Cl^-(aq)$$

The oxidation rate was found to increase approximately linearly with chloride concentration up to about 250 g/L Cl^-, at which point the rate decreased. At high enough Cl^- concentrations, the equilibrium concentration of oxygen decreases resulting in decreased reaction rate. The pH was found to have a significant effect on the oxidation rate, with significant rate increases at lower pH; the rate increase was more than expected just by the addition of more Cl^-. Yamamoto[38] found that addition of the chlorides KCl or $MgCl_2$ also increased the reaction rate.

Magalhães[37] proposed the following mechanism for the oxidation that can be combined into either of the following overall reactions in acid and base solution, respectively:

$$2\ Hg^0(\ell) + O_2(aq) + 4\ H^+ + 4\ Cl^-(aq) = 2\ HgCl_2(aq) + 2\ H_2O \quad (7)$$

$$2\ Hg^0(\ell) + O_2(aq) + 2\ H_2O + 4\ Cl^-(aq) = 2\ HgCl_2(aq) + 4\ OH^- \quad (8)$$

The overall reaction shows that O_2 is the active oxidant. This mechanism is consistent with their observation that the pH increased during the course of the reaction (due to formation of OH^-). The positive effect of lower pH and higher Cl^- is also consistent. These authors were unable to determine if the oxidation reaction occurred in solution or on the Hg^0 metal surface.

also state that the oxidation reaction may actually occur at the surface of the Hg^0 droplet and that their experiments could not distinguish between these two possibilities.

The oxidation of dissolved and liquid elemental mercury in oxygenated water with chloride present was studied by Amyot[39] The reactions were performed in the dark to eliminate photochemical reactions. The chloride present was added as KCl; no chlorine with oxidizing potential such as Cl_2 was added. Total Hg concentrations were below the solubility of Hg^0 in oxygen-free water at 25 °C (about 284 nM, or 0.057 mg/L).[7] Chloride concentrations were varied from zero to 500 μM (17.7 mg/L). In this work, oxidized Hg was considered to be the sum of Hg(I) and Hg(II) concentrations. Oxygen concentrations were maintained by contacting the stirred test solutions with air.

In solutions containing dissolved Hg^0 only with no liquid elemental Hg^0 (droplets), the rate of Hg^0 oxidation by O_2 in the presence of chloride was essentially zero. However, rapid oxidation of Hg^0 occurred when Hg metal was present. As determined by Magalhães[37], the rate of oxidation increased with increased concentration of chloride. The rate of oxidized mercury

creation was also found to be a function of the mercury droplet surface area. The oxidation rate eventually decreased due to the accumulation of oxidation products on the Hg^0 metal surface, which agrees with Magalhães' observation of calomel. The absence of O_2 resulted in no oxidation as expected.

Oxidation in the Ontario Hydro Sampling Train

Laudal[11,32] reported on tests of the Ontario Hydro sampling train,[34] which uses three impingers containing 10 wt% KCl solution to trap oxidized (Hg^{2+}) mercury. They found that the presence of Cl_2 resulted in statistically significant amounts of Hg^{2+} even though only Hg^0 was present in the test gas. They also found that the presence of SO_2 in the test gas decreased the amount oxidized. Cauch[40] specifically tested the Ontario Hydro method to quantify the effect of Cl_2 on the measured Hg^{2+}. The presence of SO_2 in the gas again eliminated the interference of Cl_2 on the Hg^{2+} measurement. Addition of sodium thiosulfate $Na_2S_2O_3$, a reducing agent, also eliminated the effect of Cl_2. Chlorine was postulated to be removed by these overall reactions:

$$SO_2 + Cl_2 + 2\,H_2O = H_2SO_4 + 2\,HCl \quad (9)$$

$$2\,Na_2S_2O_3 + Cl_2 = Na_2S_2O_6 + 2\,NaCl \quad (10)$$

Cauch[40] gave a mechanism for chorine oxidation of Hg^0:

$$Cl_2(aq) + H_2O = HClO(aq) + H^+(aq) + Cl^-(aq) \quad (11)$$

$$HOCl(aq) = H^+(aq) + OCl^-(aq) \quad (12)$$

$$Hg^o(aq) + OCl^-(aq) = Hg^{2+}(aq) + Cl^-(aq) + 2\,OH^-(aq) \quad (13)$$

Zhao[35] studied the absorption of element Hg^0 from the vapor into a solution of hypochlorite and found that the active oxidizing species was more likely to be aqueous Cl_2 rather than hypochlorite ion (OCl^-):

$$Hg^o(aq) + Cl_2(aq) \rightarrow \text{products} \quad (14)$$

For the work of both Cauch and of Zhao, aqueous Cl_2 is the more likely oxidant because low pH (high H^+) and high Cl^- both increased the rate of oxidation of Hg^0.

MODELING METHODS & RESULTS

The oxidation of elemental Hg^0 in the melter offgas system could occur in the gas phase, the liquid phase, or both. Models of homogeneous gas-phase oxidation and combined gas-phase liquid-phase reactions have been generated. A liquid-phase only model was not created because the presence of gas-phase reactions seemed highly likely. A gas-phase generation model, with HgCl is the immediate product, would appear to be most consistent with the observed formation of primarily Hg_2Cl_2 in the offgas system.

A homogeneous gas-phase oxidation model has been applied to the ESCM melter data. A combined model has also been generated to show that the gas-phase reaction product composition, when combined with the condensate composition, would result in the observed speciation of mercury.

Background

Mercury fed to DWPF melter as either Hg^0 or HgO would be volatilized as elemental mercury vapor (Hg^0) during the calcination/fusion process. The mercury vapor is then presumed to undergo oxidation reactions to either +1 or +2 oxidation state in the melter vapor space and downstream of the melter including the condensate tank. The only literature data found for mercury emission from a glass melter were taken during the ESCM tests at PNL[10], as shown in Table 2.

Homogeneous Oxidation in the Gas Phase

The mercury oxidation model was developed based on the most recent kinetic data available in the literature as described above. The model was then calibrated using the ESCM data. Specifically, only those kinetic data taken under the post-flame conditions of coal-fired power plants were used in this study mainly due to the fact that the temperature range of these data is inclusive of those typically encountered in the melter vapor space and the offgas header leading to the quencher.

Modeling Approach

With respect to the mercury speciation reactions, the ESCM and DWPF systems can be divided into three distinct reaction zones. The first (Zone 1) is the cold cap where the water portion of the slurry feed is converted into steam, and the remaining dry feed components are converted into glass and calcine gases. In this study, a high-temperature thermodynamic equilibrium software called FactSage v6.0 was used to calculate the composition of the volatile species.[41]

The calcine gases enter the second reaction zone (Zone 2) along with the elemental mercury vapor and volatile salts such as chlorides and borates of alkali metals generated in Zone 1. Zone 2 includes the vapor space of the melter and the offgas header where species volatilized from the melter mix with steam and air and further react. Reaction Zone 3 resides inside the quencher and the condensate tank (and SAS for DWPF), where steam and volatile salts are condensed and may further react in the liquid phase. It is necessary to model all three reaction zones in order to have a relatively complete description of how mercury would speciate throughout the ESCM or DWPF melter offgas system. Preliminary modeling of all three zones has been performed.

Characteristics of Offgas Carryover

The carryover of materials into the offgas can occur via two very different mechanisms: physical entrainment and vapor phase transport (or volatilization). Both feed and glassy materials can become airborne by physical entrainment aided in part by the pulling of the exhaust blower and remain as solids throughout the offgas system. Entrained particulates with mean particle size greater than 1 μm, account for much of the particle loading in the melter exhaust but over 90% of them are routinely scrubbed in the quencher.[42]

Conversely, alkali salts of chloride and borate, and elemental mercury are transported into the offgas due to their volatility at the melt temperature but later condense as offgas gets cooled and further quenched. Upon condensation, these semi-volatile salts, and any mercury salts formed, would become primarily submicron-sized aerosols that are difficult to remove using an ejector-

venturi scrubber like the DWPF quencher. As a result, the majority of the semi-volatile salts and mercury will remain in the gas stream downstream of the quencher. The peak of the particle size distribution curve shifts from > 1 μm to < 1 μm after quenching.[43] Formation of molecular HgCl supports the observation that more Hg_2Cl_2 is collected in the downstream sections of the offgas system. Hg_2Cl_2 formed from the vapor would be submicron size and pass through the quencher, whereas formation of Hg_2Cl_2 in the aqueous phase is not likely to generate these submicron particles.

Model Assumptions

The following simplifying assumptions were made to model the oxidation of mercury in the melter offgas system:

1. The composition of calcine gases produced during the melting/fusion process is at equilibrium with those of the condensed phases at 1,150 °C (Zone 1).
2. Due to thermal radiation shine, the measured melter vapor space temperature is 100 °C higher than the actual gas temperature (Zone 2).
3. The chemical components of the melter exhaust are in equilibrium at the melter vapor space gas temperature except for those chloride-containing species that are not tied to the alkali metals (Zone 2).
4. Chloride atoms that are predicted to couple with alkali metals are not available for the chlorination of mercury (Zone 2).
5. The molar ratio of Cl_2 to Cl decreases linearly with increasing temperature between 550 and 750 °C (Zone 2).

Homogeneous Gas-Phase Oxidation Model

The elementary reactions shown in Reactions (1)-(4) were used to describe the gas-phase chlorination of mercury in Zone 2. The oxidation of mercury is initiated by the Cl atoms combining with the elemental mercury vapor via Reaction (1) to form a mercurous chloride atom (+1 oxidation state). The Cl atoms can further oxidize the mercurous chloride to mercuric chloride (+2 oxidation state) via Reaction (2). Reaction (3) was added to account for the effect of temperature on the speciation of chlorine; formation of Cl_2 is favored over Cl atoms at low temperatures, while formation of Cl atoms is favored at high temperatures. The formation of Cl_2 by the recombination of Cl atoms by Reaction (4)), which would slow down Reactions (1) and (2) and accelerate Reaction (3), was excluded from the model, since its rate constant is many orders of magnitude smaller than the other reactions and the concentration of Cl atoms not be high enough to overcome such a large deficit in the rate constant.

The 2nd order rate constants used in the model were taken from a recent study using the laser photolysis/laser induced fluorescence (LP/LIF) technique.[14] It is noted that the upper temperature bounds for the rate constants of Reactions (1) to (3) are 50 and 100 °C lower than the estimated gas temperatures in the ESCM vapor space (Test 3) and the DWPF melter vapor space, respectively. As stated earlier, the temperature ranges are low because they were specifically derived under the post-flame conditions of coal-fired power plants. It is implicitly assumed here that these rate constants can be extrapolated to the temperature regions of interest to this study.

The concentrations of [Hg], [HgCl], [$HgCl_2$], [Cl] and [Cl_2] were found as a function of time by solving the following five rate equations simultaneously:

$$\frac{d[Hg]}{dt} = -k_1[Hg][Cl] \quad (15)$$

$$\frac{d[Cl]}{dt} = -k_1[Hg][Cl] - k_2[HgCl][Cl] + k_3[HgCl][Cl_2] \quad (16)$$

$$\frac{d[HgCl]}{dt} = k_1[Hg][Cl] - k_2[HgCl][Cl] - k_3[HgCl][Cl_2] \quad (17)$$

$$\frac{d[HgCl_2]}{dt} = k_2[HgCl][Cl] + k_3[HgCl][Cl_2] \quad (18)$$

$$\frac{d[Cl_2]}{dt} = -k_3[HgCl][Cl_2] \quad (19)$$

All of the mercury fed is volatilized, so the initial concentration of mercury, $[Hg]_o$, is known, and both $[HgCl]_o$ and $[HgCl_2]_o$ are zero. Therefore, in order to solve Eqs. (15)-(19), the initial concentrations of [Cl] and $[Cl_2]$ must be known, and the strategy used to find $[Cl]_o$ and $[Cl_2]_o$ is as follows:

1. Run the FactSage model to calculate the equilibrium melter exhaust composition at the measured melter vapor space temperature.
2. Calculate the total Cl atoms that are predicted not to couple with alkali metals (non-alkali Cl), e.g., HCl, Cl, Cl_2, $HgCl_2$, etc:

   $[HCl]+[Cl]+[Cl_2]+[HgCl_2]+[HgCl]$
3. Calculate the equilibrium Cl_2/Cl ratio predicted by the FactSage model.
4. Assume a fraction of the total non-alkali Cl atoms calculated in step 2 that exist as either Cl or Cl_2:

   $$\frac{[Cl]+[Cl_2]}{[HCl]+[Cl]+[Cl_2]+[HgCl_2]+[HgCl]} \equiv \%Clx$$
5. Assume a percent approach to the equilibrium Cl_2/Cl ratio from step 3.
6. Solve for $[Cl]_o$ and $[Cl_2]_o$ based on the assumed values from steps 4 and 5.
7. Run Zone 2 oxidation model.
8. Check if the calculated HgCl/$HgCl_2$ ratio matches the experimental data.
9. If not, repeat steps 4-8.

The five ordinary differential equations of the Zone 2 kinetic model were solved simultaneously using the RK4 v3.0 program.[44] The reasoning behind taking a percent approach to the equilibrium Cl_2/Cl ratio in step 5 is that the equilibrium prediction of Cl_2 concentration will be much higher than the actual value based in part on the kinetics of its formation, as evidenced by the negligibly small rate constant for Reaction (4). So, the initial Cl_2/Cl ratio is reduced to a certain percentage of what is predicted by the equilibrium model. This procedure was used to model the ESCM Test 1 and Test 3 data.

To model the DWPF offgas system, the same steps were followed, except:

- For steps 1-3, DWPF conditions at 650 ^oC vapor space temperature were used.

- The fraction of the non-alkali Cl atoms that exist as Cl or Cl_2 (step 4) was set to the average of the values found for the two ESCM tests.
- The percent approach to equilibrium Cl_2/Cl ratio (step 5) was set to the average of the values found for the two ESCM tests.
- In step 7, the DWPF conditions were used.

The basis for using the average ESCM values is the fact that the DWPF melter vapor space temperature of 650 °C falls exactly in the middle of the ESCM test temperatures.

Modeling of ESCM Tests

The results of Zone 1 and 2 model runs are presented in this section along with their implications on the DWPF melter offgas system operation. It should be noted that these results and discussions are only preliminary and scoping in nature. Further substantiation of these results would require a more in-depth modeling study accompanied by the proof-of-the-principle experimental tests.

The Zone 2 models of the ESCM tests contain two critical parameters pertaining to the partitioning of Cl/Cl_2 among non alkali-metal binding chloride atoms. The values of these parameters were determined by matching the calculated insoluble-to-soluble mercury ratios (Hg_2Cl_2/$HgCl_2$) with the measured data:

	Test 1	Test 3
Target Hg_2Cl_2/$HgCl_2$ (mole/mole)	9 : 1	1 : 1

ESCM Zone 1 Model

The input compositions for the FactSage equilibrium model are given in Table 3. The two main differences between Tests 1 and 3 were that (1) the melter was fed 2.8 times faster during Test 1 than Test 3 and (2) the melter vapor space was kept 200 ^{o}C cooler during Test 3 by turning off the vapor space heaters. The rate of melter air inleakage was the same at 25 kg/hr in both tests. The molar ratio of Cl/Hg was 12, which means that regarding the chlorination of mercury, chloride was present in excess.

The results of the FactSage model runs at 1150 °C are shown in Table 4. As expected, 100% of the mercury fed was predicted to volatilize as elemental mercury vapor. At 1150 °C under equilibrium conditions, 100% of the chloride fed was also predicted to volatilize as either HCl or alkali chlorides at a ratio of 40:60. A negligible quantity of Cl atoms was also predicted to form but not Cl_2. It should be noted that the mercury and alkali chlorides became part of the offgas carryovers due to their low vapor pressures at the melt temperature, and the model predictions do not include any solids that are physically entrained because such a prediction is beyond the scope of an equilibrium model.

ESCM Zone 2 Model

The Zone 2 model consisted of two parts. The first was the FactSage model to calculate the equilibrium compositions of the melter exhausts at the measured melter vapor space temperatures of 750 and 550 ^{o}C for Tests 1 and 3, respectively. The second part was the gas-phase kinetics model of mercury chlorination which further adjusted the equilibrium speciation

of mercury. The input for the Zone 2 FactSage model included; (1) the ideal-gas output shown in Table 4, (2) free H_2O that volatilizes from the cold cap, and (3) the air inleakage to the melter.

The results of the FactSage model runs are shown in Table 5 under the heading Equilibrium. As in the Zone 1 run at 1150 °C, the 60:40 split of total chloride atoms between HCl and alkali metals, respectively, was generally maintained in Test 1, while at 200 °C lower in Test 3 equilibrium favors ~10% more chloride atoms to couple with alkali metals. The summary of gas-phase results given in Table 5 also show that equilibrium favors (1) all of the chloride atoms that do not couple with alkali metals to be in the form of HCl with little or no Cl/Cl_2, and (2) the formation of Cl_2 over Cl even at 750 °C. This is why the adjustment steps for the fraction ($Cl+Cl_2$) and the approach to equilibrium were necessary to force some of the equilibrium-predicted HCl into Cl and Cl_2 for the mercury chlorination reactions to proceed.

After a few trial-and-error runs, it was found that when the %Clx fraction was set at 13.5%, and the percent approach to the equilibrium Cl_2/Cl ratio set at 1%, the calculated $HgCl/HgCl_2$ ratio would match the experimental value of 9:1 at these initial concentrations, as shown in Figure 4. These results are summarized in Table 6. The kinetics of mercury chlorination are so fast that the reactions are essentially complete in 0.5 ms. Therefore, considering the fact that the estimated gas residence time in the ESCM vapor space was on the order of 5 seconds for Test 1, it may be concluded that the chlorination of mercury will be complete at the instant Cl and Cl_2 are formed. However, this study does not address the question of how atomic Cl and Cl_2 are formed in the first place.

Table 3 Input Compositions of ESCM Tests 1 and 3 Feeds for FactSage Model

Insoluble Solids	Test 1 mol/hr	Test 3 mol/hr	Soluble Solids	Test 1 mol/hr	Test 3 mol/hr
SiO2	16.0	5.71	NaCOOH	0.902	0.322
Li2O	3.10	1.11	Mn(COOH)2	0.438	0.157
Na2O	2.81	1.00	NaNO3	0.314	0.112
Fe(OH)3	2.45	0.876	Ca(COOH)2	0.209	0.0747
B2O3	1.91	0.681	NaCl	0.185	0.0662
Al(OH)3	1.58	0.565	KCOOH	0.0400	0.0143
MgO	0.329	0.118	NaF	0.0151	0.00540
MnO2	0.187	0.0669	Na2SO4	0.0118	0.00423
Zeolite	0.184	0.0657	CsNO3	0.0107	0.00384
Al2O3	0.184	0.0657	Sr(COOH)2	0.00429	0.00153
Ni(OH)2	0.173	0.0619			
ZrO2	0.108	0.0385			
CaCO3	0.0523	0.0187			
CaSO4	0.0247	0.00883			
Cr(OH)3	0.0243	0.00868			
RuO2	0.0199	0.00712			
Hg	0.0155	0.00552			
CaF2	0.0153	0.00547			
Cu2O	0.0141	0.00504			
Ca3(PO4)2	0.00313	0.00112			

Table 4 FactSage Equilibrium Model Results at 1,150 °C for ESCM Tests.

GASES	Test1 mol/hr	Test 3 mol/hr	GASES	Test1 mol/hr	Test 3 mol/hr	GLASS COMPONENTS	Test1 mol/hr	Test 3 mol/hr
H2O	7.05	2.53	LiF	4.68E-04	0	MgO	0.329	0.118
CO2	2.07	0.772	OBF	3.39E-04	0	MnO	0.626	0.224
H2	0.186	0.0668	LiOH	3.33E-04	1.23E-04	Na2O	3.03	1.09
N2	0.162	0.0579	(HBO2)3	1.75E-04	5.84E-05	SiO2	10.4	3.73
CO	0.122	0.0454	Fe(OH)2	1.40E-04	5.03E-05	CaO	0.249	0.102
HCl	**0.0736**	**0.0258**	NaF	1.34E-04	0	Al2O3	0.974	0.348
NaCl	**0.0662**	**0.0239**	NaOH	1.20E-04	4.41E-05	K2O	0	0.00709
HF	0.0447	0	SO	8.51E-05	3.07E-05	NiO	0.0811	0.0260
LiCl	**0.0309**	**0.0111**	**KCl**	**0**	**8.01E-05**	Fe2O3	0.0412	0.0124
SO2	0.0217	0.00783	**NiCl2**	**5.10E-05**	**1.75E-05**	B2O3	1.12	0.400
HBO2	0.0169	0.00593	KBO2	0	3.19E-05	MnSO4	1.14E-07	4.46E-08
Hg	**0.0155**	**0.00552**	COS	2.86E-05	1.06E-05	NiSO4	1.48E-08	5.18E-09
H3BO3	0.0110	0.00385	HS	2.09E-05	7.53E-06	Fe2(SO4)3	7.49E-09	2.47E-09
LiBO2	0.00996	0.00359	**CsOH**	**1.78E-05**	**6.56E-06**	Na2SO4	5.52E-07	2.17E-07
CsCl	**0.00756**	**0.00271**	S2	1.67E-05	6.01E-06	CaSO4	4.53E-08	2.04E-08
NaBO2	0.00707	0.00255	**MnCl2**	**1.66E-05**	**6.17E-06**	MgSO4	5.99E-08	2.34E-08
CsBO2	0.00309	0.00111	Na	1.58E-05	5.85E-06	Li2Si2O5	2.78	0.986
(NaCl)2	**0.00249**	**8.98E-04**	Ni(OH)2	1.11E-05	4.00E-06	FeO	1.01	0.385
H2S	0.00132	4.76E-04	**(CsCl)2**	**8.57E-06**	**3.07E-06**	NaBO2	0.921	0.317
FeCl2	**5.33E-04**	**1.83E-04**	**Cl**	**2.90E-06**	**1.02E-06**	LiBO2	0.592	0.228
(LiCl)2	**5.14E-04**	**1.86E-04**	B2O3	1.30E-06	4.46E-07	Fe3O4	0.454	0.155
						Ni	0.0723	0.0289
						Ni3S2	0.00663	0.00234

Table 5 Results of Zone 2 FactSage and Kinetic Model Runs for ESCM Tests.

ESCM Run	Test 1	Test 1	Test 3	Test 3
Calculation Mode	Equilibrium	Kinetic	Equilibrium	Kinetic
Melter Vapor Space Gas Temperature (°C)	650	650	450	450
GASES	mol/hr	mol/hr	mol/hr	mol/hr
H2O	152	152	54.4	54.4
N2	20.0	20.0	19.9	19.9
O2	5.12	5.12	5.22	5.22
CO2	2.20	2.20	0.818	0.818
HCl	0.106	0.0947	0.0242	0.0282
HF	0.0447	0.0447	0	0
H3BO3	0.0381	0.0381	0.0170	0.0170
Hg	0.0136	0.00183	6.73E-06	8.08E-04
CsCl	0.00782	0.00782	1.18E-05	1.18E-05
HgCl	0	0.0120	0	0.00239
HgCl2	0.00165	0.00137	0.00552	0.00233
(CsCl)2	0.00141	0.00141	4.04E-06	4.04E-06
NaCl	0.00123	0.00123	1.95E-07	1.95E-07
LiCl	8.96E-04	8.96E-04	2.49E-07	2.49E-07
(NaCl)2	3.95E-04	3.95E-04	2.94E-08	2.94E-08
NO	3.54E-04	3.54E-04	1.37E-05	1.37E-05
HgO	2.70E-04	2.70E-04	4.18E-07	4.18E-07
(LiCl)2	2.38E-04	2.38E-04	6.28E-08	6.28E-08
NO2	1.24E-05	1.24E-05	5.98E-06	5.98E-06
(HBO2)3	1.32E-05	1.32E-05	9.55E-06	9.55E-06
Cl2	7.69E-06	5.76E-07	1.40E-05	3.23E-11
OH	7.46E-06	7.46E-06	1.07E-08	1.07E-08
Cl	4.13E-06	3.11E-06	4.32E-08	3.15E-11
SOLIDS	mole/hr	mole/hr	mole/hr	mole/hr
NaCl (s)	0.0597	0.0597	0.0267	0.0267
LiNa(SO4) (s)	0.0165	0.0165	0.00153	0.00153
LiBO2 (s)	0.00985	0.00985	0	0
Li2SO4 (s)	0.00652	0.00652	0.00678	0.00678
CsCl (s)	0	0	0.00380	0.00380

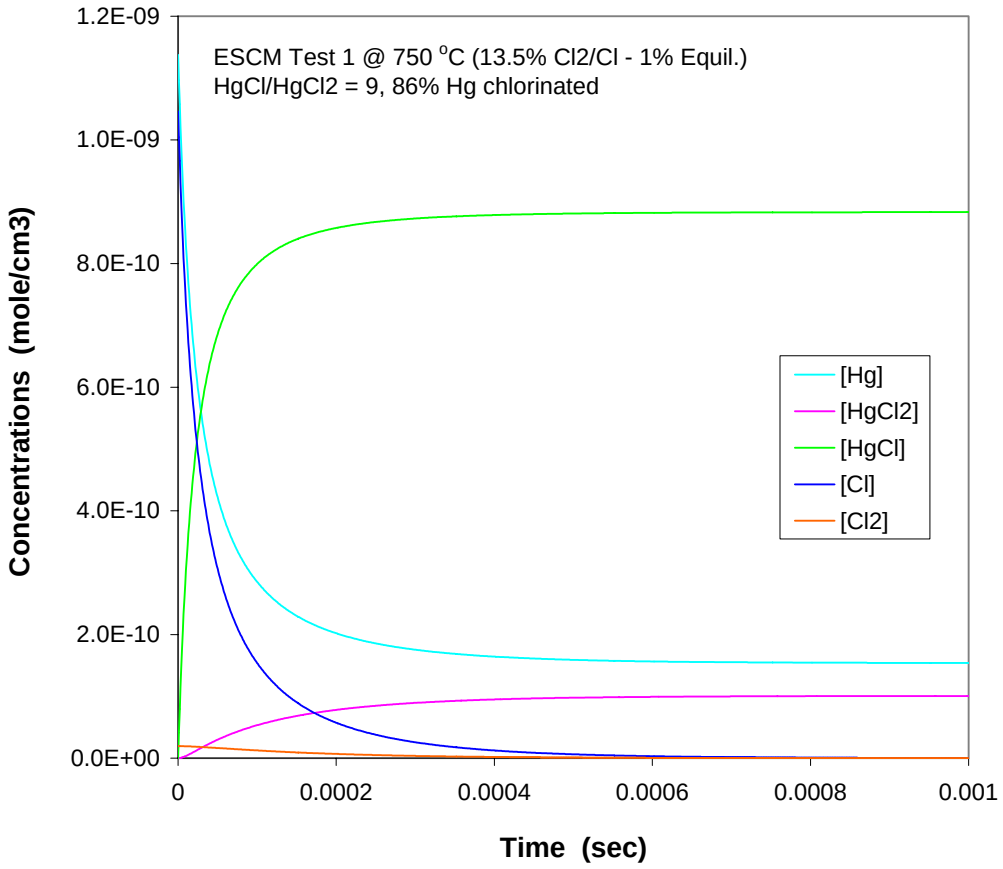

Figure 4 Concentration Profiles of Mercury Chlorination Reactants and Products for ESCM Test 1

Similarly for Test 3, it was found that when the %Clx was set at 20%, and the percent approach to the equilibrium Cl_2/Cl ratio set at 0.22%, the calculated HgCl/$HgCl_2$ ratio would match the experimental value of 1:1 at these initial concentrations. As expected, the resulting initial concentration of Cl for Test 3 was calculated to be lower than that for Test 1, while the resulting initial concentration of Cl_2 was higher than its counterpart for Test 1, since the temperature was lower during Test 3. It is interesting to note that the calculated percent total Cl atoms not tied to the alkali metals that exist as either Cl atom or Cl_2 increased from 13.5 to 20%, as the temperature was decreased from Test 1 to Test 3. This is due to the fact that the formation of Cl_2 is favored over that of Cl atom at lower temperatures, and the net effect is to increase the number of total Cl atoms in both Cl and Cl_2. These results are summarized in Table 6. Note that for both Tests 1 and 3, the total chlorinated Hg was about 86%; the remaining Hg was predicted to be Hg^0 and HgO.

Figure 5 shows that the calculated HgCl/$HgCl_2$ ratio matches the experimental value of 1:1 at these initial concentrations of Cl and Cl_2. Due to a lower temperature, it took about three times as long to complete the chlorination reactions as in Test 1. However, the reactions were still complete in 0.15 ms, which is four orders of magnitude shorter than the estimated gas residence time of 14 seconds for Test 3. This confirms the earlier conclusion that the chlorination of mercury will be complete at the instant Cl and Cl_2 are formed. The model also predicted that at

the Cl/Hg ratio of 12, 85% of the mercury fed was chlorinated either to HgCl or $HgCl_2$ in both ESCM tests.

Table 6 Summary of Homogeneous Oxidation Model Parameters for ESCM Tests

ESCM Run	Test 1	Test 1	Test 3	Test 3
Calculation Mode	Equilibrium	Kinetic	Equilibrium	Kinetic
% Cl tied to alkali metals	40.3	40.3	46.4	46.4
% Cl not tied to alkali metals (%Clx)	59.7	59.7	53.6	53.6
% Cl as $Cl+Cl_2$ in non-alkali Cl	0.0178	13.5	0.0795	20.0
% Approach to equilibrium	-	1.00	-	0.22
Ratio Cl as Cl_2/Cl atom	3.72	0.0372	647	1.42
Initial conc $[Cl]_o$ (mole/cm3)	3.03E-13	1.05E-09	9.06E-15	6.09E-10
Initial conc $[Cl_2]_o$ (mole/cm3)	5.64E-13	1.95E-11	2.93E-12	4.33E-10
Calculated $HgCl/HgCl_2$	0	8.77	0	1.03
Target $HgCl/HgCl_2$	-	9.00	-	1.00
Chlorinated Hg (% total Hg)	12.4	86.5	99.9	85.4

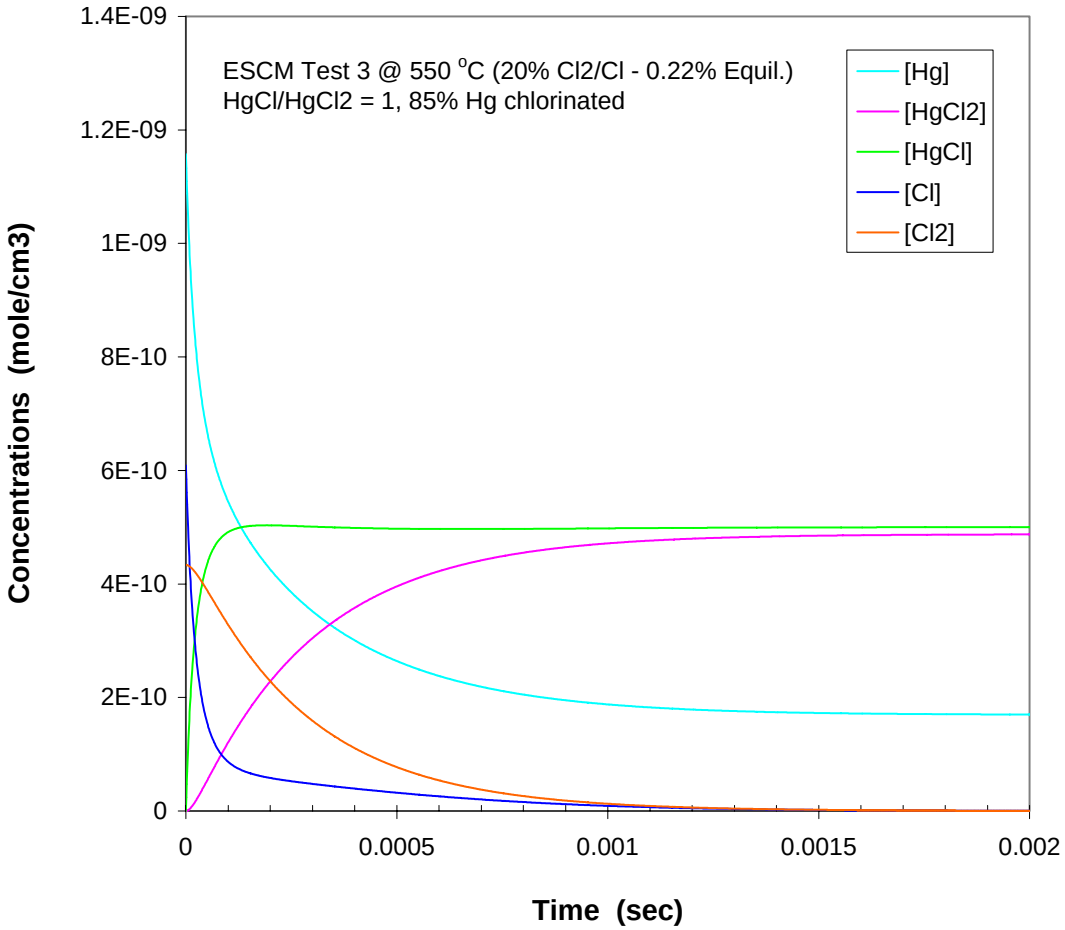

Figure 5 Concentration Profiles of Mercury Chlorination Reactants and Products for ESCM Test 3.

Modeling of DWPF

The goal of the ESCM modeling was to determine: (1) the percent total Cl atoms not tied to the alkali metals that exist as either Cl atom or Cl_2, and (2) the percent approach to the equilibrium Cl_2/Cl ratio at different temperatures. Now, with the values of these critical parameters determined at 650 and 450 °C gas temperatures, the same Zone 1 and 2 models were run under DWPF conditions.

DWPF Zone 1 Model

The composition of the DWPF melter feed with no mercury removal is shown in Table 7. The molar Cl-to-Hg ratio is only 0.4, compared to 12 for the ESCM feeds, which means that there is a significant deficit in chloride so the overall conversion of elemental mercury into HgCl and/or $HgCl_2$ is expected to be very low.

The results of the FactSage model run at 1150 ^{o}C are shown in Table 8. As expected, 100% of the mercury fed as HgO was predicted to volatilize as elemental mercury vapor. At 1,150 ^{o}C under equilibrium conditions, 100% of the chloride fed was also predicted to volatilize as either HCl or alkali chlorides at a ratio of 25:75, respectively. Notice that the percent total Cl atoms that couple with alkali metals was predicted to be much higher than for the ESCM feeds. Perhaps due to a significant shortage of chloride atoms, neither Cl atoms nor Cl_2 were predicted to form at any concentrations. As with the ESCM results, these model predictions do not include any physically-entrained solids.

Table 7 Composition of DWPF Melter Feed with No Hg Removal.

Insoluble Solids	lb/hr	mol/hr	Soluble Solids	lb/hr	mol/hr
SiO2	101	764	NaCOOH	32.2	215
FeOOH	29.1	148	NaNO3	17.7	94.5
B2O3	19.8	129	Mn(COOH)2	10.1	31.5
Al(OH)3	18.6	108	UO2(COOH)2	4.68	5.89
Na2O	11.3	82.8	Ca(COOH)2	2.89	10.1
Li2O	11.3	172	HCOOH	1.19	11.7
AlOOH	9.54	72.1	Ni(COOH)2	1.06	3.22
HgO	2.86	5.99	Mg(COOH)2	0.785	3.12
Ni(OH)2	2.63	12.9	KNO3	0.361	1.62
Mg(OH)2	1.60	12.5	NaCl	0.302	2.34
Ca(OH)2	0.960	5.88	Na2SO4	0.0659	0.210
MnO2	0.671	3.50	Cu(COOH)2	0.00488	0.0144
CaSO4	0.579	1.93	La(COOH)3	0.00381	0.00631
Ca3(PO4)2	0.520	0.760	Zn(COOH)2	0.00345	0.0101
Coal	0.149	5.64			
Cr(OH)3	0.0339	0.149			
RhO2	0.0274	0.0920			
RuO2	0.0252	0.0861			
BaSO4	0.0229	0.0446			
Ce(OH)3	0.0176	0.0418			
Cu(OH)2	0.0124	0.0577			
La(OH)3	0.0106	0.0252			
TiO2	0.00891	0.0506			
Zn(OH)2	0.00882	0.0402			
PuO2	0.00661	0.0111			

PdO	9.63E-04	0.00357

Table 8 FactSage Equilibrium Model Results at 1,150 °C for DWPF SB5 Run.

GASES	mol/hr	GASES	mol/hr	GLASS COMPONENTS	mol/hr	GLASS COMPONENTS	mol/hr
H2O	462	LiOH	0.0496	SiO2	454	CaO	17.9
CO2	321	NaOH	0.0178	Na2O	173	MgO	15.6
N2	48.1	Fe(OH)2	0.00918	Li2Si2O5	126	Ni	13.8
CO	18.9	(NaCl)2	0.00893	LiBO2	90.1	Si2O4	5.74
H2	12.2	KBO2	0.00891	NaBO2	81.4	NiO	2.17
Hg	5.99	SO	0.00756	FeO	69.9	K2O	0.802
UO3	4.95	KCl	0.00449	Al2O3	66.5	Fe2O3	0.628
SO2	1.93	COS	0.00442	NaAlSiO4	47.3	Ni3S2	0.0508
NaCl	1.18	Na	0.00275	B2O3	42.0	Na2SO4	1.73E-04
UO3(H2O)	0.938	(LiCl)2	0.00184	MnO	35.0	MnSO4	3.50E-05
LiBO2	0.886	HS	0.00160	Fe3O4	25.8	CaSO4	1.79E-05
HBO2	0.661	S2	0.00148			MgSO4	1.56E-05
NaBO2	0.629	(HBO2)3	0.00133			NiSO4	2.17E-06
HCl	0.579	Ni(OH)2	7.30E-04			K2SO4	8.01E-07
LiCl	0.551	UO2Cl2	7.05E-04			Fe2(SO4)3	6.28E-07
H3BO3	0.318	H	6.84E-04				
H2S	0.0868	OH	5.79E-04				
		FeCl2	5.03E-04				

DWPF Zone 2 Model

As with the ESCM case, the DWPF Zone 2 model consisted of two parts. The first was the FactSage model to calculate the equilibrium compositions of the melter exhausts at the measured melter vapor space temperatures of 650 °C. The second part was the gas-phase kinetics model of mercury chlorination which further adjusted the equilibrium speciation of mercury. The input for the Zone 2 FactSage model included:

(1) the ideal-gas output shown in Table 8,
(2) free H_2O that volatilizes from the cold cap,
(3) the melter air inleakage and purge.

The results of the Zone 2 FactSage model runs for DWPF are shown in Table 9 under the heading Equilibrium. One notable result is that the percent total Cl atoms predicted to exist as alkali chlorides decreased from 75% of the total chloride fed at 1,150 °C to zero as the melter exhaust was cooled below 850 °C. By contrast, the percent total Cl atoms predicted to exist as alkali chlorides were 35-40% even at lower temperatures for the ESCM feeds. The summary of gas-phase results also shows that equilibrium favors: (1) nearly 65% of the total chloride fed to oxidize the mercury, (2) much of the remaining 35% to be in the form of HCl, and (3) the formation of Cl_2 over Cl at 550 °C actual gas temperature at a ratio of nearly 6:1.

Since the nominal DWPF melter vapor space temperature was right at the midpoint of the two ESCM temperatures, the percent total Cl atoms not tied to the alkali metals that exist either as Cl atom or Cl_2 was set at 16.75%, which is the average of the two corresponding ESCM values.

Likewise, the percent approach to the equilibrium Cl_2/Cl ratio was set at 0.61%, which is again the average of the two corresponding ESCM values. At the calculated initial concentrations of Cl and Cl_2, the calculated $HgCl/HgCl_2$ ratio was 53, which means that >98% of the chlorinated mercury would have an oxidation state of +1. These values are summarized in Table 10. Also note that with so few Cl atoms available compared to Hg, the reactions are essentially complete in 0.03 ms, and only 6% of the mercury fed would be chlorinated. As shown in Table 9, the remaining 94% of the mercury fed would exist as either Hg^0 (90%) or HgO (4%).

The measured chloride level in a recent DWPF feed sample is actually an order of magnitude lower than that of the test case used in this study. As a result, the degree of shortage in chloride in relation to mercury will be even greater in future DWPF operations. This would make the predicted level of HgCl in the actual melter exhaust less than 6% of the total mercury fed, while that of elemental mercury is expected to be greater than 90%. Therefore, much of the mercury fed will likely condense as the elemental mercury in the offgas system.

Table 9 Results of Zone 2 FactSage and Kinetic Model Runs for DWPF SB5.

Calculation Mode	**Equilibrium**	**Kinetic**
Melter Vapor Space Gas Temperature (°C)	**550**	**550**
GASES	**mol/hr**	**mol/hr**
H2O	9095	9095
N2	4620	4620
O2	1198	1198
CO2	340	340
Hg	5.00	5.38
H3BO3	2.50	2.50
HCl	0.812	1.95
HgCl2	0.763	0.00709
SO3	0.300	0.300
HgO	0.227	0.227
SO2	0.0467	0.0467
NO	0.0197	0.0197
O2S(OH)2	0.00815	0.00815
NO2	0.00289	0.00289
(HBO2)3	0.00115	0.00115
OH	5.27E-05	5.27E-05
HBO2	4.11E-05	4.11E-05
Cl2	3.17E-05	4.87E-04
HOCl	2.43E-05	2.43E-05
Cl	1.09E-05	6.60E-06
Hg2	6.19E-06	6.19E-06
HgCl	7.33E-07	0.376
KCl	6.76E-07	6.76E-07
NaCl	3.62E-07	3.62E-07
SOLIDS	mole/hr	mole/hr
UO3 (s)	5.89	5.89
LiNa(SO4) (s)	1.48	1.48
Na2SO4 (s)	0.186	0.186

KLi(SO4) (s)	0.0134	0.0134
Fe2O3 (s)	0.00459	0.00459

Table 10 Summary of Homogeneous Oxidation Model Parameters for DWPF

Calculation Mode	Equilibrium	Kinetic
% Cl tied to alkali metals	1.55E-05	1.55E-05
% Cl not tied to alkali metals	100.0	100.0
% Cl as Cl+Cl2 in non-alkali Cl (%Clx)	0.00318	16.8
% Approach to equilibrium	-	0.61
Ratio Cl as Cl_2/Cl atom	5.83	0.0356
Initial conc $[Cl]_o$ (mole/cm3)	1.06E-14	3.67E-10
Initial conc $[Cl2]_o$ (mole/cm3)	3.08E-14	6.53E-12
Calculated HgCl/$HgCl_2$	9.60E-07	53.1
Chlorinated Hg (% total Hg)	12.7	6.41

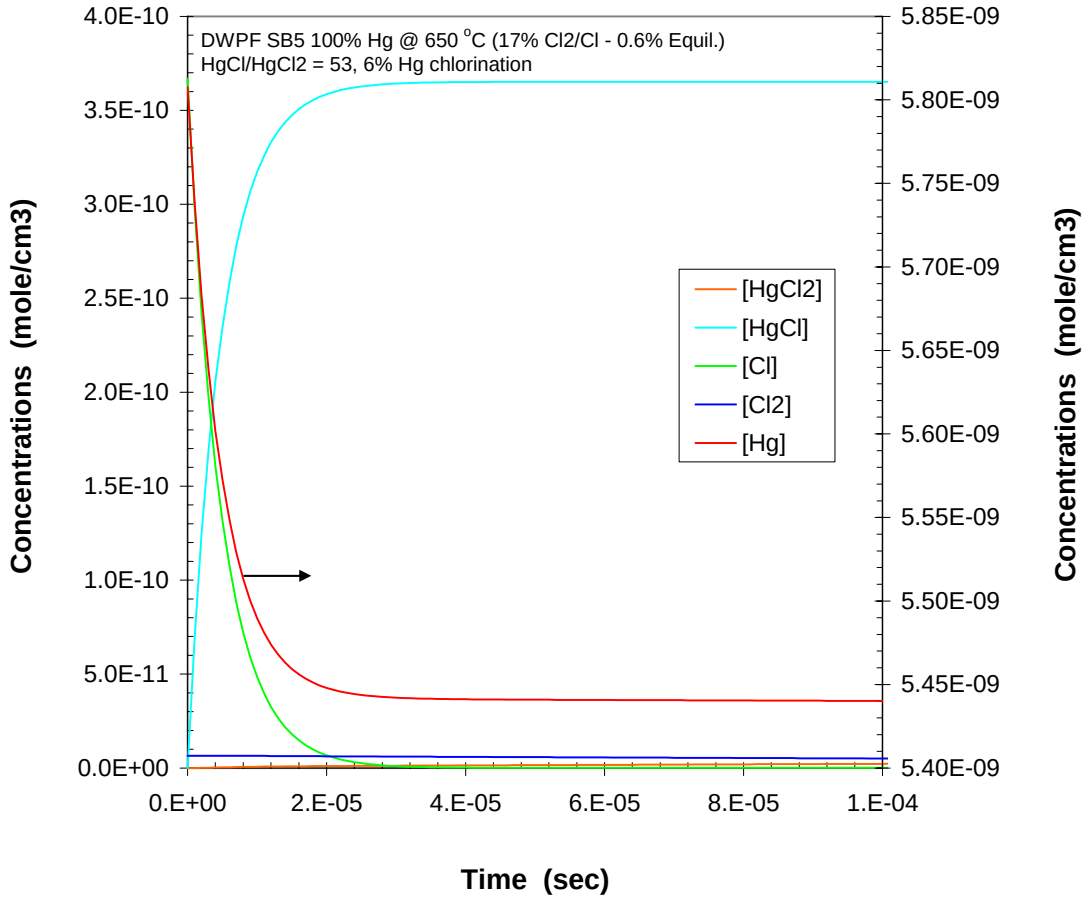

Figure 6. Concentration Profiles of Mercury Chlorination Reactants and Products for DWPF SB5 Feed with Zero Mercury Removal in CPC.

Equilibria and Reactions in Aqueous Solutions

Modeling of the aqueous reactions and equilibria was performed using the StreamAnalyzer™ aqueous simulation software from OLI Systems, Inc.[45] The OLI Public database and the aqueous thermodynamics framework were used. A Private database was generated to correct an error in the Hg_2Cl_2 solubility constant.

Equilibria

The aqueous equilibria of Hg^0, Hg^{2+} and Hg_2^{2+} compounds at 25 °C predicted using the OLI software were compared to the best values tabulated in the literature to validate the use of the OLI software. [6-9,45-47] The equilibrium constants calculated using StreamAnalyzer, after accounting for species activity coefficients, matched most of the tabulated values (generally for infinite dilution) within the same order of magnitude. The typical discrepancy was a factor of about 2, but factors of up to about 6 were found for some reactions. This level of agreement is within the range of values reported in the literature by different authors.

The solubility and Henry's law constants as functions of temperature for Hg^0 and $HgCl_2$ were generated using StreamAnalyzer and these values were compared to literature values. The solubility and predicted vapor pressure for Hg^0 deviated from the literature by up to a factor of 2. The solubility at 25 °C was predicted to be 1.3×10^{-7} mol/kg versus the accepted value of about 2.85×10^{-7} mol/kg.[7]

The solubility of $HgCl_2$ is predicted accurately by OLI, but the vapor pressure is 4-7 times higher than given in the literature. Fortunately, the concentration of $HgCl_2$ in the present work is expected to be low, so errors in the vapor pressure should not have a significant effect on the results.

Aqueous Redox Reactions

The OLI software has the capability of handling some reduction-oxidation (redox) reactions in the aqueous phase. This redox capability is equilibrium based, so there is no consideration for reaction kinetics. In StreamAnalyzer, redox reactions can be turned on or off for individual elements. (In the discussion below, anions are always assumed to be aqueous (aq).)

Oxidizers present in the melter offgas are Cl_2, O_2, NO, and NO_2. The roles of NO and NO_2 in Hg chemistry are not clear. Sulfur dioxide SO_2 can oxidize Hg^0, but can also reduce Hg^{2+}. It has been shown that SO_2 can suppress the oxidation of Hg^0 by Cl_2 by reducing Cl_2 to Cl^-.[40] Hydrochloric acid HCl is not an oxidizer, but provides chloride to the equilibria with oxidized Hg (as does NaCl and other chlorides). In the reactions below, the oxidation states of the elements are shown above the reactions.

Elemental Hg Oxidation by Oxygen

$$2\,Hg(\ell) + O_2(aq) = 2\,HgO(s) \qquad (20)$$

This reaction takes place in solution between Hg^0 liquid metal and dissolved oxygen. In the OLI software with Hg redox turned on, oxygen always oxidizes Hg. In actual tests, O_2 does not appreciably oxidize Hg^0 unless Cl^- is present.[37,39] In the presence of less than stoichiometric O_2 and with Cl^- present, Hg^0 can be partially oxidized to the +1 oxidation state (Hg_2^{2+}).

A shortcoming of the OLI software is that it applies equilibrium between all phases, so the large excess of O_2 in an offgas stream effectively oxidizes all oxidizable species in solution even if there are actually reaction kinetics or mass transfer limitations. Therefore, to handle the actually limited oxidizing power of O_2 in this situation, the amount of O_2 must be limited. At any time, the amount of O_2 in solution cannot exceed its solubility, so that limiting the transfer of O_2 from the gas to the aqueous phase should be a method for limiting oxidation by O_2.

Mercuric oxide solid can react with chloride ions to give mercuric chloride:

$$HgO(s) + 2\ Cl^- + H_2O = HgCl_2(aq) + 2\ OH^- \quad (21)$$

This is not a redox reaction; it probably proceeds through the slightly soluble $Hg(OH)_2$. The presence of Cl^- produces the more stable $HgCl_2$ from the $Hg(OH)_2$.

Elemental Hg Oxidation by Chlorine

$$Hg^o(\ell) + Cl_2(aq) = HgCl_2(aq) \quad (22)$$

This reaction probably does not occur as written by this stoichiometry, but by a more complex series of reactions. Less than stoichiometric amounts of Cl_2, like O_2, result in partial oxidation of Hg^0 to the +1 oxidation state. The dissolution of Cl_2 in water is a disproportionation that forms hypochlorous acid (HOCl) and HCl, which are in the +1 and -1 oxidations states, respectively:

$$Cl_2(aq) + H_2O = HOCl(aq) + H^+ + Cl^- \quad (23)$$

Chlorine can also oxidize water to form O_2, as shown by this overall reaction:

$$2\ Cl_2(aq) + 2\ H_2O = 4\ H^+ + 4\ Cl^- + O_2 \quad (24)$$

With Cl redox turned on, OLI's equilibrium calculations always result in any excess Cl_2 reacting with water to form O_2, which may be thermodynamically favorable, but not kinetically significant.

Reactions with SO_2

Generally, SO_2 acts a reductant for most species of interest, but in some cases appears to increase the amount of Hg^0 oxidized. Hutson[36] has shown that in scrubbing of Hg^0 using $NaClO_2$ as an oxidant, the addition of some SO_2 to the vapor enhances scrubbing and oxidation of Hg^0, but that higher concentrations of SO_2 then result in less scrubbing and oxidation. Scott[48] has shown that SO_2 {S(IV)}can reduce Hg^{2+} to Hg^0 in both the gas and liquid phases and that one of the products in addition to Hg^0 is the oxidized species HgS, which results from disproportionation of the S(IV) species. Such a reaction could be:

$$3\ Hg^{+2} + 6\ SO_2 + 8\ H_2O = 2\ Hg^0 + HgS + 5\ H_2SO_4 + 2H^+ \quad (25)$$

Zhao[49] has shown that SO_2 inhibits the oxidation of Hg^0 by Cl species in the gas phase when water is present, but that no inhibition occurs when water is absent. In aqueous solutions, the formation of an Hg•S(IV) intermediate complex followed by decomposition to form Hg^0 has been proposed to explain the reemission of Hg as Hg^0 from scrubbers that remove Hg^{2+}.

Sulfur dioxide will act as a reductant for oxidized mercury or chlorine. In OLI, Cl_2 and SO_2 preferentially and thus Cl_2 does not oxidize Hg^0. This redox chemistry reflects the actual

experimentally determined chemistry. Cauch[40] showed that SO_2 reduces Cl_2 to chloride in solution, while sulfur is apparently oxidized to sulfuric acid:

$$Cl_2 + SO_2 + 2\ H_2O = 2\ HCl + H_2SO_4 \quad (26)$$

However, excess SO_2 in OLI can oxidize Hg^0 to HgS, while sulfur itself disproportionates to S(-2) and S(+6), as shown in Reaction (27). This reaction does not appear to actually occur in real systems.

$$Hg^0 + 3\ SO_2 + 2\ H_2O = HgS + 2\ H_2SO_4 \quad (27)$$

Therefore, like O_2, the effect of sulfur redox in OLI must be carefully checked. In OLI, with S redox turned on, SO_2 in water disproportionates into elemental sulfur S_8 and sulfuric acid, H_2SO_4:

$$24\ SO_2 + 16\ H_2O = S_8 + 16\ H_2SO_4 \quad (28)$$

Although this reaction may be thermodynamically favorable, the dissolution of SO_2 into water actually gives sulfurous acid:

$$SO_2 + H_2O = H_2SO_3 \quad (29)$$

Combined Homogeneous Gas Phase and Liquid Phase Oxidation – ESCM Tests

The homogeneous vapor-phase oxidation results from the FactSage modeling of Tests 1 and 3 were used as inputs to an approximate liquid-phase model. This composition did not contain any entrained glass or feed. For the results from both tests, the offgas composition was cooled to 25 °C, resulting in aqueous condensate, a gas phase, and precipitated Hg species. Because of the effect of O_2 on the redox of mercury, the O_2 in these streams was converted mole-for-mole to inert N_2. The OLI model input species are shown in Table 11. Species specific to FactSage that are not valid species in OLI were adjusted as shown. For the OLI input, the phase does not matter, so the gas phase and condensed phase species were added.

Table 11 FactSage Output and Input to OLI Aqueous Model

	ESCM Test 1 FactSage Equil+Kinetic	OLI Input Adjusted	ESCM Test 3 FactSage Equil+Kinetic	OLI Input Adjusted
Vapor	mol/h	mol/h	mol/h	mol/h
H_2O	1.52E+02	1.52E+02	5.44E+01	5.44E+01
N_2	2.00E+01	2.52E+01	1.99E+01	2.52E+01
O_2	5.12E+00	0	5.22E+00	0
CO_2	2.20E+00	2.20E+00	8.18E-01	8.18E-01
HCl	9.47E-02	9.47E-02	2.82E-02	2.82E-02
HF	4.47E-02	4.47E-02	0.00E+00	0.00E+00
H_3BO_3	3.81E-02	3.81E-02	1.70E-02	1.70E-02
CsCl	7.82E-03	1.06E-02	1.18E-05	3.82E-03
Hg	1.83E-03	1.83E-03	8.08E-04	8.08E-04
HgCl	1.20E-02	1.20E-02	2.39E-03	2.39E-03
$HgCl_2$	1.37E-03	1.37E-03	2.33E-03	2.33E-03
HgO	2.70E-04	2.70E-04	4.18E-07	4.18E-07
Hg(I)	%	77.6	%	43.2
Hg(II)		10.6		42.2
Hg(0)		11.8		14.6
$(CsCl)_2$	1.41E-03	CsCl above	4.04E-06	CsCl above
NaCl	1.23E-03	6.17E-02	1.95E-07	2.67E-02
LiCl	8.96E-04	1.37E-03	2.49E-07	3.74E-07
$(NaCl)_2$	3.95E-04	NaCl above	2.94E-08	NaCl above
NO	3.54E-04	3.54E-04	1.37E-05	1.37E-05
$(LiCl)_2$	2.38E-04	LiCl above	6.28E-08	LiCl above
NO_2	1.24E-05	1.24E-05	5.98E-06	5.98E-06
$(HBO2)_3$	1.32E-05	none	9.55E-06	none
Cl_2	5.76E-07	2.13E-06	3.23E-11	4.81E-11
OH	7.46E-06	none	1.07E-08	none
Cl	3.11E-06	Cl_2 above	3.15E-11	Cl_2 above
Condensed				
NaCl	5.97E-02	NaCl above	2.67E-02	NaCl above
$LiNaSO_4$	1.65E-02	$Li_2SO_4 + Na_2SO_4$	1.53E-03	$Li_2SO_4 + Na_2SO_4$
Na_2SO_4	none	8.27E-03	none	7.67E-04
$LiBO_2$	9.85E-03	9.85E-03	0.00E+00	0.00E+00
Li_2SO_4	6.52E-03	1.48E-02	6.78E-03	7.54E-03
CsCl	0.00E+00	CsCl above	3.80E-03	CsCl above

The pH of actual DWPF condensate samples is approximately 2-2.5, so the pH was adjusted to 2.5 in the aqueous models by adding NaOH. The pH without adjustment was about 1.6. The temperature and pressure were assumed to be 25 °C and 1 atm. Ambient temperature was chosen because even though the condensate tank temperature was higher, the samples were cooled to room temperature before analysis, so the actual speciation measured would be that at room temperature.

The target ratios of the mercury species are shown in the first column of Table 12. The FactSage output is shown in the second column. The third column shows the OLI model output using the inputs from Table 11. For both tests, the amount of Hg(I) is over-predicted. Because the

proportion of chlorine present as Cl_2 at the quench temperature of around 45-60 °C will be higher than those in Table 11 (at 650 and 450 °C), the amount of Cl_2 was adjusted in the OLI model. In Table 12, the predicted mercury speciation for the best-fit Cl_2 amount for both tests is shown in the column A; values using the average Cl_2 are shown in column B. The original and adjusted amounts of Cl_2 are shown in the bottom two rows. For both cases, increasing the Cl_2 amount to around 0.27 mM gives mercury speciation that matches the target values. This very small aqueous concentration of Cl_2 is quite reasonable. In future work, the Cl_2 concentration entering the quencher, after cooling, will be calculated using FactSage.

Table 12 Product Percentages for ESCM Test Model

			Hg_2^{2+} : Hg^{2+} : Hg^0		
				A	**B**
ESCM Test	**Condensate Target**	**FactSage Output and OLI Input**	**OLI Predicted, No Cl_2 Adjustment**	**OLI Predicted, each Test's Cl_2 Adjusted Individually**	**OLI Predicted, Cl_2 Adjusted to Same for Both Tests**
1	90 : 10 : ~0	77 : 11 : 12	99 : 0 : 1	90 : 10 : 0	92 : 8 : 0
3	50 : 50 : ~0	43 : 42 : 15	73 : 27 : 0	50 : 50 : 0	46 : 54 : 0
1	Cl_2 Amount (mM):		7.77×10^{-4}	0.32	0.27
3	Cl_2 Amount (mM):		1.76×10^{-8}	0.23	0.27

The calculation scheme and results are presented in a flow diagram in Figure 7.

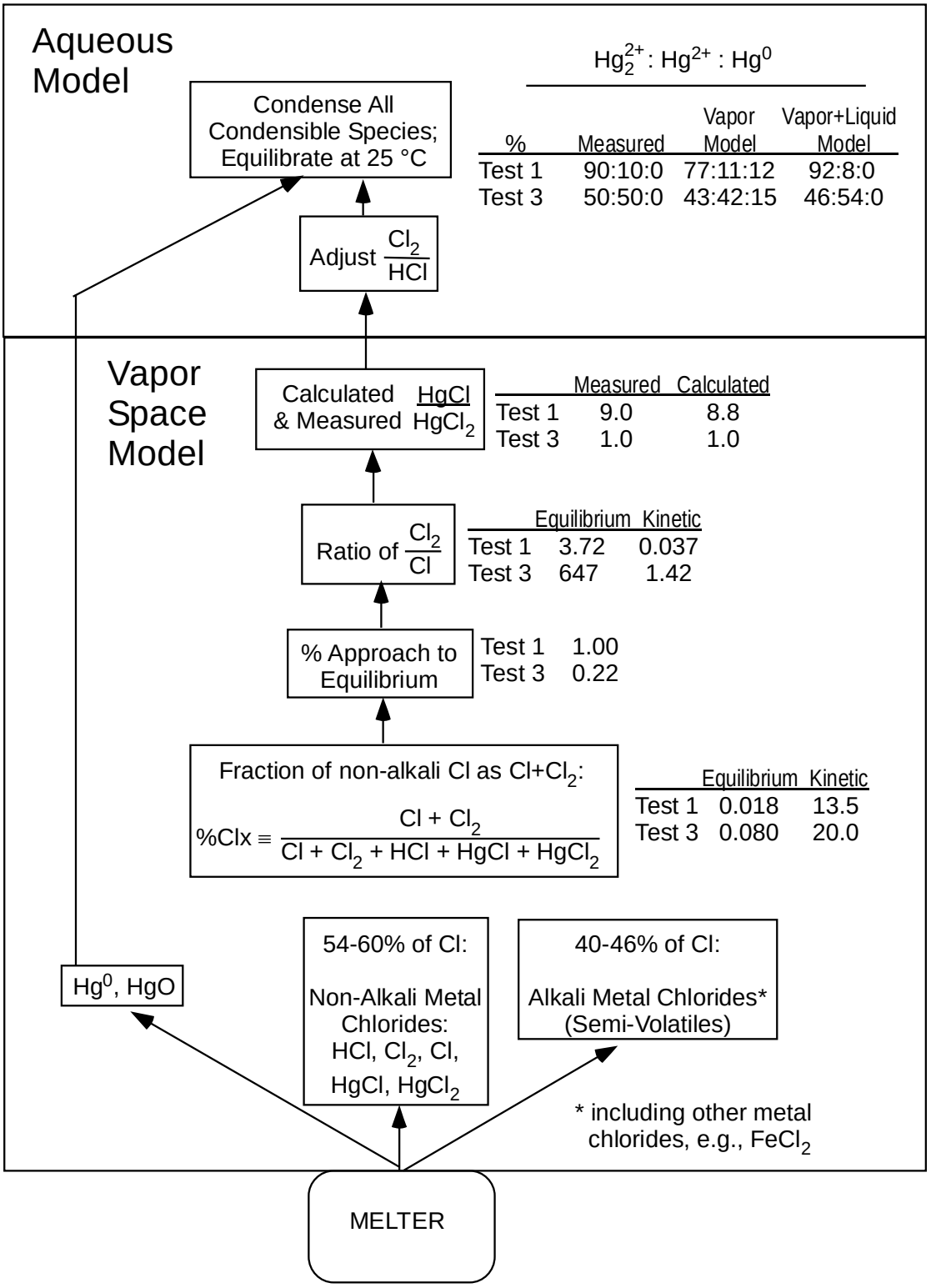

Figure 7 Flow Diagram of Calculation Scheme

In future work, the FactSage model will be used to predict the actual amount of chlorine present at the quencher inlet temperature.

CONCLUSIONS

A homogeneous gas-phase oxidation model was developed to study the speciation of mercury in the DWPF melter offgas system. The model contains two critical parameters pertaining to the partitioning of chloride among HCl, Cl, Cl_2, and alkali chlorides in the melter vapor space, and their values were determined at two different melter vapor space temperatures by matching the predicted molar ratio of HgCl to $HgCl_2$ with those measured during the ESCM tests. The calibrated model was then run for DWPF conditions, where no mercury removal from the feed was assumed, so the Cl-to-Hg ratio in the melter feed was only 0.4. The results of the model show that due to excessive shortage of chloride, only 6% of the mercury fed is expected to get chlorinated, mostly as Hg_2Cl_2, while the remaining mercury would exist either as elemental mercury (90%) or HgO (4%).

The aqueous chemistry model was shown to to predict the mercury speciation in the condensate for a simple one-step condensation. With the assumption of a Cl_2 concentration in the condensate of 0.27 mM, the elemental Hg^0 and HgO in the vapor were converted to oxidized Hg and the Hg_2^{2+} to Hg^{2+} ratios matched the measured ratios very closely.

There are many process benefits to be gained by skipping the mercury stripping step. This study was initiated to determine what impact zero mercury removal in the CPC would have on the melter offgas system. This study was intended to be scoping in nature, so the results presented are only preliminary. Further substantiation of these results to support implementation in the plant would require a more in-depth modeling study of all three reaction zones, including the aqueous-phase reactions in the offgas system. With much of the mercury fed to the melter expected to be present as elemental mercury vapor at the quencher inlet, it would be necessary to look into the mechanism of mercury condensation, e.g., whether elemental mercury would have a tendency to coat available solid surfaces or form droplets and, if they form droplets, how mercury droplets grow in size. Ensuing theoretical predictions must then be validated with proof-of-principle experiments.

REFERENCES

1. M.R. Norton, H.B. Shah, M.E. Stone, L.E. Johnson, and R. O'Driscoll, "Overview - Defense Waste Processing Facility Operating Experience," Report No. USDOE WSRC-MS-2002-00145, 2002.

2. N.D. Hutson, J.R. Zamecnik, M.E. Smith, D.H. Miller, and J.A. Ritter, "Integrated DWPF Melter System (IDMS) Campaign Report - Mercury Operation," Report No. USDOE WSRC-TR-91-0363, 1991.

3. N.E. Bibler, "Characterization of Three Samples Taken from the Off Gas System of DWPF Melter One," Report No. USDOE WSRC-TR-2003-00423, 2003.

4. K. Zeigler and N. Ned Bibler, "Characterization of DWPF Melter Off-Gas Quencher and Steam Atomized Scrubber Deposit Samples," Report No. USDOE WSRC-STI-2007-00262, 2007.

5. T.L. Fellinger, "Results for the DWPF Slurry Mix Evaporator Condensate Tank, Off Gas Condensate Tank, and Recycle Collection Tank Samples," Report No. USDOE WSRC-TR-2004-00577, 2004.

6. R.D. Eddy and A.W.C. Menzies, "The Solubilities of Certain Inorganic Compounds in Ordinary Water and in Deuterium Water," *The Journal of Physical Chemistry,* **44** [2] 207-35 (1940).

7. H.L. Clever, S.A. Johnson, and M.E. Derrick, "The Solubility of Mercury and Some Sparingly Soluble Mercury Salts in Water and Aqueous-Electrolyte Solutions," *J. Phys. Chem. Ref. Data,* **14** [3] 631-81 (1985).

8. L.G. Hepler and G. Olofsson, "Mercury - Thermodynamic Properties, Chemical-Equilibria, and Standard Potentials," *Chem. Rev.,* **75** [5] 585-602 (1975).

9. O.S. Pokrovsky, "Experimental-Determination of the Association Constant of Mercurous Ion with Chloride in Aqueous-Solutions at 20-80-Degrees-C," *Geokhimiya,* [6] 881-94 (1995).

10. R.W. Goles, G.J. Sevigny, and C.M. Andersen, "LFCM (Liquid-Fed Ceramic Melter) Processing Characteristics of Mercury," Report No. PNL-SA-17928; CONF-900809-5, 1990.

11. D. Laudal, B. Nott, T. Brown, and R. Roberson, "Mercury Speciation Methods for Utility Flue Gas," *Fresenius. J. Anal. Chem.,* **358** [3] 397-400 (1997).

12. R.N. Sliger, J.C. Kramlich, and N.M. Marinov, "Towards the Development of a Chemical Kinetic Model for the Homogeneous Oxidation of Mercury by Chlorine Species," *Fuel Processing Technology,* **65-66** 423-38 (2000).

13. M.H. Mendelsohn and C.D. Livengood, "Critical Review of Mercury Chemistry in Flue Gas," Report No. USDOE ANL/ESD/06-4, 2006.

14. P.H. Taylor, R. Mallipeddi, and T. Yamada, "LP/LIF Study of the Formation and Consumption of Mercury(I) Chloride: Kinetics of Mercury Chlorination," *Chemosphere,* **61** [5] 685-92 (2005).

15. D.G. Horne, R. Gosavi, and O.P. Strausz, "Reactions of Metal Atoms. I. The Combination of Mercury and Chlorine Atoms and the Dimerization of HgCl," *The Journal of Chemical Physics,* **48** [10] 4758-64 (1968).

16. M.H. Xu, Y. Qiao, C.G. Zheng, L.C. Li, and J. Liu, "Modeling of Homogeneous Mercury Speciation Using Detailed Chemical Kinetics," *Combust. Flame,* **132** [1-2] 208-18 (2003).

17. C.L. Senior, A.F. Sarofim, T. Zeng, J.J. Helble, and R. Mamani-Paco, "Gas-Phase Transformations of Mercury in Coal-Fired Power Plants," *Fuel Processing Technology,* **63** [2-3] 197-213 (2000).

18. B. Hall, P. Schager, and O. Lindqvist, "Chemical-Reactions of Mercury in Combustion Flue-Gases," *Water Air Soil Pollut.,* **56** 3-14 (1991).

19. J.R. Edwards, R.K. Srivastava, and J.D. Kilgroe, "A Study of Gas-Phase Mercury Speciation Using Detailed Chemical Kinetics," *J. Air Waste Manage. Assoc.,* **51** [6] 869-77 (2001).

20. S. Niksa, J.J. Helble, and N. Fujiwara, "Kinetic Modeling of Homogeneous Mercury Oxidation: The Importance of N O and H_2O in Predicting Oxidation in Coal-Derived Systems," *Environ. Sci. Technol.,* **35** [18] 3701-6 (2001).

21. A. Fry, B. Cauch, G.D. Silcox, J.S. Lighty, and C.L. Senior, "Experimental Evaluation of the Effects of Quench Rate and Quartz Surface Area on Homogeneous Mercury Oxidation," *Proceedings of the Combustion Institute,* **31** 2855-61 (2007).

22. K.C. Galbreath, C.J. Zygarlicke, E.S. Olson, J.H. Pavlish, and D.L. Toman, "Evaluating Mercury Transformation Mechanisms in a Laboratory - Scale Combustion System," *Sci. Total Environ.,* **261** [1-3] 149-55 (2000).

23. B. Hall, P. Schager, and J. Weesmaa, "The Homogeneous Gas-Phase Reaction of Mercury with Oxygen, and the Corresponding Heterogeneous Reactions in the Presence of Activated Carbon and Fly-Ash," *Chemosphere,* **30** [4] 611-27 (1995).

24. B. Hall, O. Lindqvist, and E. Ljungstrom, "Mercury Chemistry in Simulated Flue-Gases Related to Waste Incineration Conditions," *Environ. Sci. Technol.,* **24** [1] 108-11 (1990).

25. G.A. Norton, H.Q. Yang, R.C. Brown, D.L. Laudal, G.E. Dunham, and J. Erjavec, "Heterogeneous Oxidation of Mercury in Simulated Post Combustion Conditions," *Fuel,* **82** [2] 107-16 (2003).

26. K. Schofield, "Mercury Emission Chemistry: The Similarities or Are They Generalities of Mercury and Alkali Combustion Deposition Processes?," *Proceedings of the Combustion Institute,* **30** [1] 1263-71 (2005).

27. K. Schofield, "New Method to Minimize High-Temperature Corrosion Resulting from Alkali Sulfate and Chloride Deposition in Combustion Systems. II. Molybdenum Salts," *Energy Fuels,* **19** [5] 1898-905 (2005).

28. K. Schofield, "Let Them Eat Fish: Hold the Mercury," *Chemical Physics Letters,* **386** [1-3] 65-9 (2004).

29. P.A. Ariya, A. Khalizov, and A. Gidas, "Reactions of Gaseous Mercury with Atomic and Molecular Halogens: Kinetics, Product Studies, and Atmospheric Implications," *The Journal of Physical Chemistry A,* **106** [32] 7310-20 (2002).

30. C.J. Lin and S.O. Pehkonen, "The Chemistry of Atmospheric Mercury: A Review," *Atmospheric Environment,* **33** [13] 2067-79 (1999).

31. N.Q. Yan, S.H. Liu, S.G. Chang, and C. Miller, "Method for the Study of Gaseous Oxidants for the Oxidation of Mercury Gas," *Industrial & Engineering Chemistry Research,* **44** [15] 5567-74 (2005).

32. D.L. Laudal, T.D. Brown, and B.R. Nott, "Effects of Flue Gas Constituents on Mercury Speciation," *Fuel Processing Technology,* **65** 157-65 (2000).

33. C.L. Senior, L.E. Bool, G.P. Huffman, and F.E. Huggins, "A Fundamental Investigation of Toxic Substances from Coal Combustion," *Abstr. Pap. Am. Chem. Soc.,* **212** 7-FUEL (1996).

34. "Standard Test Method for Elemental, Oxidized, Particle-Bound and Total Mercury in Flue Gas Generated from Coal-Fired Stationary Sources (Ontario Hydro Method)," ASTM International, ASTM D 6784 - 02, 2008.

35. L.L. Zhao and G.T. Rochelle, "Mercury Absorption in Aqueous Hypochlorite," *Chem. Eng. Sci.,* **54** [5] 655-62 (1999).

36. N.D. Hutson, R. Krzyzynska, and R.K. Srivastava, "Simultaneous Removal of SO_2, NO_x, and Hg from Coal Flue Gas Using a $NaClO_2$-Enhanced Wet Scrubber," *Industrial & Engineering Chemistry Research,* **47** [16] 5825-31 (2008).

37. M.E.A. de Magalhães and M. Tubino, "A Possible Path for Mercury in Biological-Systems - the Oxidation of Metallic Mercury by Molecular-Oxygen in Aqueous-Solutions," *Sci. Total Environ.,* **170** [3] 229-39 (1995).

38. M. Yamamoto, "Stimulation of Elemental Mercury Oxidation in the Presence of Chloride Ion in Aquatic Environments," *Chemosphere,* **32** [6] 1217-24 (1996).

39. M. Amyot, F.M.M. Morel, and P.A. Ariya, "Dark Oxidation of Dissolved and Liquid Elemental Mercury in Aquatic Environments," *Environ. Sci. Technol.,* **39** [1] 110-4 (2005).

40. B. Cauch, G.D. Silcox, J.S. Lighty, J.O.L. Wendt, A. Fry, and C.L. Senior, "Confounding Effects of Aqueous-Phase Impinger Chemistry on Apparent Oxidation of Mercury in Flue Gases," *Environ. Sci. Technol.,* **42** [7] 2594-9 (2008).

41. Factsage© Version 6.0, Thermfact/CRCT, Montreal, QC Canada, 2009, www.crct.polymtl.ca.

42. W.P. Colven, "Off-Gas System Data Summary for the Ninth Run of the Large Slurry Fed Melter," Report No. USDOE DPST-83-809, 1983.

43. D.M. Sabatino, J.L. Kessler, and W.P. Colven, "Summary of the Eighth Run of the Large Slurry Fed Melter," Report No. USDOE DPST-83-915, 1983.

44. T. Co, RK4 Version 3.0 4th-Order Runge-Kutta Solver, Michigan Technological University, Houghton, MI, 2005.

45. Streamanalyzer 2.0.63, OLI Systems, Inc., Morris Plains, NJ, 2008.

46. Solubility Data Series, Vol. 29, *Mercury in Liquids, Compressed Gases, Molten Salts and Other Elements*. Edited by H.L. Clever, M. Iwamoto, S.H. Johnson, and H. Miyamoto. Pergamon Press, Oxford, 1987.

47. Y. Marcus, "Compilation and Evaluation of Solubility Data in the Mercury (U) Chloride-Water System," *J. Phys. Chem. Ref. Data,* **9** [4] 1307-29 (1980).

48. S.L. Scott, H. Yusuf, N. Lahoutifard, and K. Maunder (2003). Homogeneous and Heterogeneous Reactions of Atmospheric Mercury(II) with Sulfur(Iv), E D P Sciences.

49. Y.X. Zhao, M.D. Mann, E.S. Olson, J.H. Pavlish, and G.E. Dunham, "Effects of Sulfur Dioxide and Nitric Oxide on Mercury Oxidation and Reduction under Homogeneous Conditions," *J. Air Waste Manage. Assoc.*, **56** [5] 628-35 (2006).